DRD Line Item No. SE- 6

DOE/JPL-954929-79/5

INVESTIGATION OF RELIABILITY ATTRIBUTES AND ACCELERATED STRESS FACTORS ON TERRESTRIAL SOLAR CELLS

FIFTH QUARTERLY REPORT

J.W. Lathrop and J.L. Prince

Department of Electrical and Computer Engineering

Clemson University

Clemson, SC, 29631

15 JULY, 1979

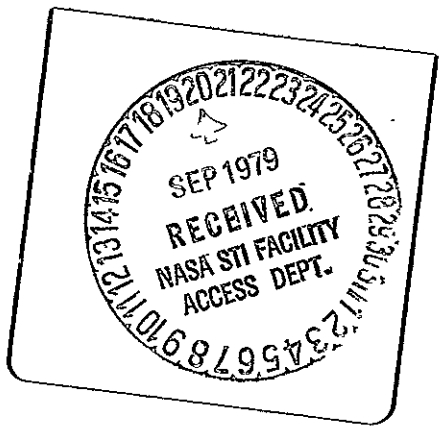

PREPARED FOR
JET PROPULSION LABORATORY

PREPARED BY
CLEMSON UNIVERSITY, CLEMSON, SOUTH CAROLINA 29631

DRD Line Item No. SE-6 DOE/JPL - 954929-79/5

ENGINEERING AREA

INVESTIGATION OF RELIABILITY ATTRIBUTES AND ACCELERATED STRESS FACTORS ON TERRESTRIAL SOLAR CELLS

FIFTH QUARTERLY REPORT

9 March 1979 - 1 July 1979

J.W. Lathrop and J.L. Prince

15 July, 1979

The JPL Low-Cost Silicon Solar Array Project is sponsored by the U.S. Department of Energy and forms part of the Solar Photovoltaic Conversion Program to initiate a major effort toward the development of low-cost solar arrays. This work was performed for the Jet Propulsion Laboratory, California Institute of Technology by agreement between NASA and DoE.

ABSTRACT

Results obtained during the reporting period on the program "Investigation of Reliability Attributes and Accelerated Stress Factors on Terrestrial Solar Cells" include the definition of a simplified stress test schedule for terrestrial solar cells based on the work performed during the first program year, and the design and fabrication of improved jigs and fixtures for electrical measurement and stress testing. Implementation of these advanced techniques for accelerated stress testing is underway on three solar cell types different from the cell types investigated in the first year's program. In addition, review of the literature on second quadrant phenomena was begun and some preliminary second-quadrant electrical measurements were performed. Results obtained at the first down time for 75°C B-T testing and biased and unbiased T-H pressure cooker testing of type F cells showed little or no degradation in electrical parameters. Significant physical effects (large solder bubbles) were noted for type F cells subjected to the pressure cooker stress test.

TABLE OF CONTENTS

LIST OF FIGURES

LIST OF FIGURES

(continued)

LIST OF TABLES

1.0 INTRODUCTION

1.1 Program Objective and Approach

The objective of this study is to perform investigations of factors involved in the reliability of terrestrial solar cells, to study in a preliminary fashion second quadrant effects in terrestrial solar cells, and to develop a plan for disseminating reliability information within the photovoltaic community.

Reliability characteristics of the basic solar cells intended for terrestrial application will be a key factor in determining whether national goals for solar photovoltaic power generation are met in a timely fashion. Prior to the inception of this program, very little was known concerning the nature of the time-to-failure (TTF) distributions of solar cells in terrestrial ambient conditions, the failure modes and failure mechanisms which control the TTF distributions, the appropriate methods for accelerated stress testing for reliability verification, or the process modifications which might be required to upgrade reliability performance. The program reported on here represents the second year of effort to define these reliability attributes for individual, unencapsulated terrestrial solar cell devices. The program is intended not merely to establish the base-line reliability for present state-of-the-art cells, but to also establish the methodology to both permit intercomparison of available cells and permit evaluation of cell structures which will be developed in the future. In this second year of effort three cell types, different from the four types investigated in the first year effort, are being studied. Some characteristics of these cell types are shown in Table 1.1.

Cell Type	Thickness (mils)	Size (in)	Substrate Material	Junction Type	Anti-Reflective Coating	Metalization	Surface Characteristics
F	12-14	3.9 x .8 rectangular	EFG Si	n/p diffused	Si_3N_4	Cr-Ti-Ag + PbSnAg Solder	"smooth"
G	12 nominal	3 dia.	Czochralski Si	n/p diffused	Si_3N_4	Pd-Ni + PbSn Solder	textured
H	12 nominal	2 x 2 square	Polycrystalline Si	n/p implanted	TiO_2	Ti-Pd-Ag	"smooth"

Table 1.1. Physical Characteristics of Cells Studies in Second Year of Program.

The stress testing approach is different from that taken earlier in that no preliminary stress testing experiments were planned for the current effort. Instead, the first measurement/inspection downtime in each stress test is being included somewhat earlier than "normal" and based on results from this downtime, subsequent downtimes will be fixed. Thus in a sense the experiments will be incorporated into the body of the large scale testing program.

The approach to the investigation of second quadrant effects is to perform a thorough literature review, and to perform some preliminary second quadrant measurements on selected samples. The measurements will be circumscribed by experimental capability and instrument availability, and are not intended to constitute a thorough investigation of second quadrant effects. Based on results and analysis a second quadrant characterization procedure will be recommended.

1.2 Program Personnel

Personnel who worked on the project during the first quarter were:

Dr. J.W. Lathrop - Professor

Dr. J.L. Prince - Professor

Dr. F.W. Morgan - Assistant Professor

Mr. R.A. Hartman - Graduate Student

Mr. K. Labib - Graduate Student

Mr. C. Saylor - Graduate Student

Mr. F. Christ - Graduate Student

2.0 TECHNICAL DISCUSSION

2.1 Electrical Measurements

The electrical measurement technique used for the 3 new cell types (F,G,H) is basically the same as for the previous cell types (A,B,C,E). Figure 2.1 is an overall view of the new measurement system. This equilibrium measurement technique has been discussed in detail in previous quarterly and annual reports. However, while the basic technique remained the same, some changes were made to the jigs and to the light source.

The light source was redesigned as shown in Figure 2.2 to make the changing of bulbs easier and to facilitate alignment of the light pattern. An elapsed time indicator was installed in the control panel so that a running record could be kept concerning bulb life. Average bulb life appears at this point to be 60 to 100 hours. The new bulb mounts incorporated a 3-point adjustment mechanism which permitted each bulb to be independently tilted. The intent was to achieve a more constant profile over the cell area. In actuality, however, tilting the bulbs appeared to have only limited effect on the profile, probably due to the long reflective barrel. Nevertheless, a completely satisfactory profile was achieved, with a maximum variation of $\pm$ 2.5% across the cell field. Furthermore, this intensity variation was obtained without the use of a diffuser such as was used on the A,B,C, and E cells.

The cell holder was modified to use a common vacuum chamber with individual water cooled contacting plates for each cell type. Figure 2.3 is a photograph of the jig assembly for the rectangular F-cell. As with earlier jigs this one incorporates a spring loaded

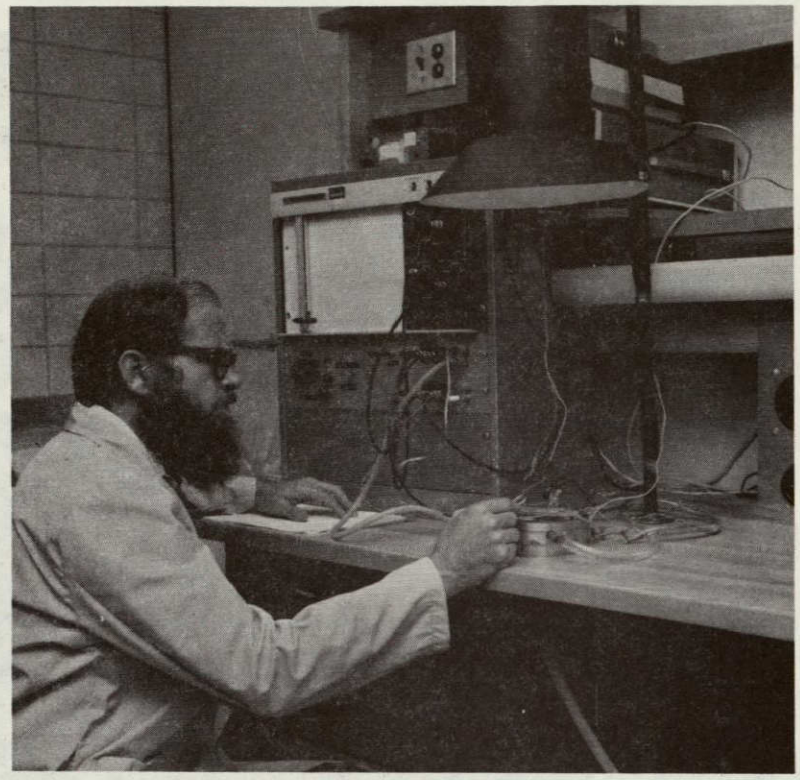

Figure 2.1 Overall View of Electrical Measurement System

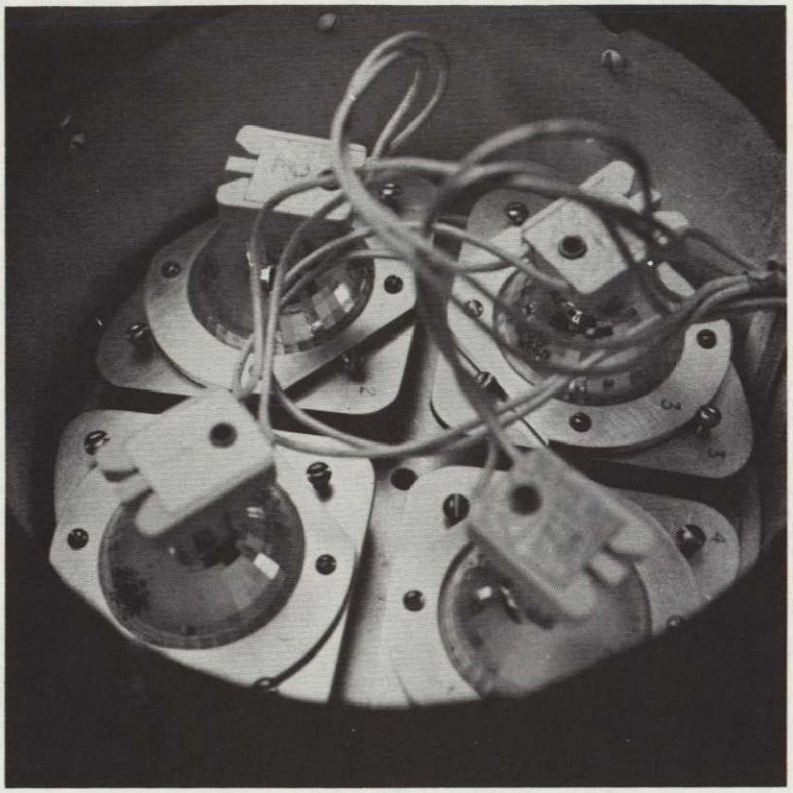

Figure 2.2 Improved Arrangement of Bulbs in New Light Source

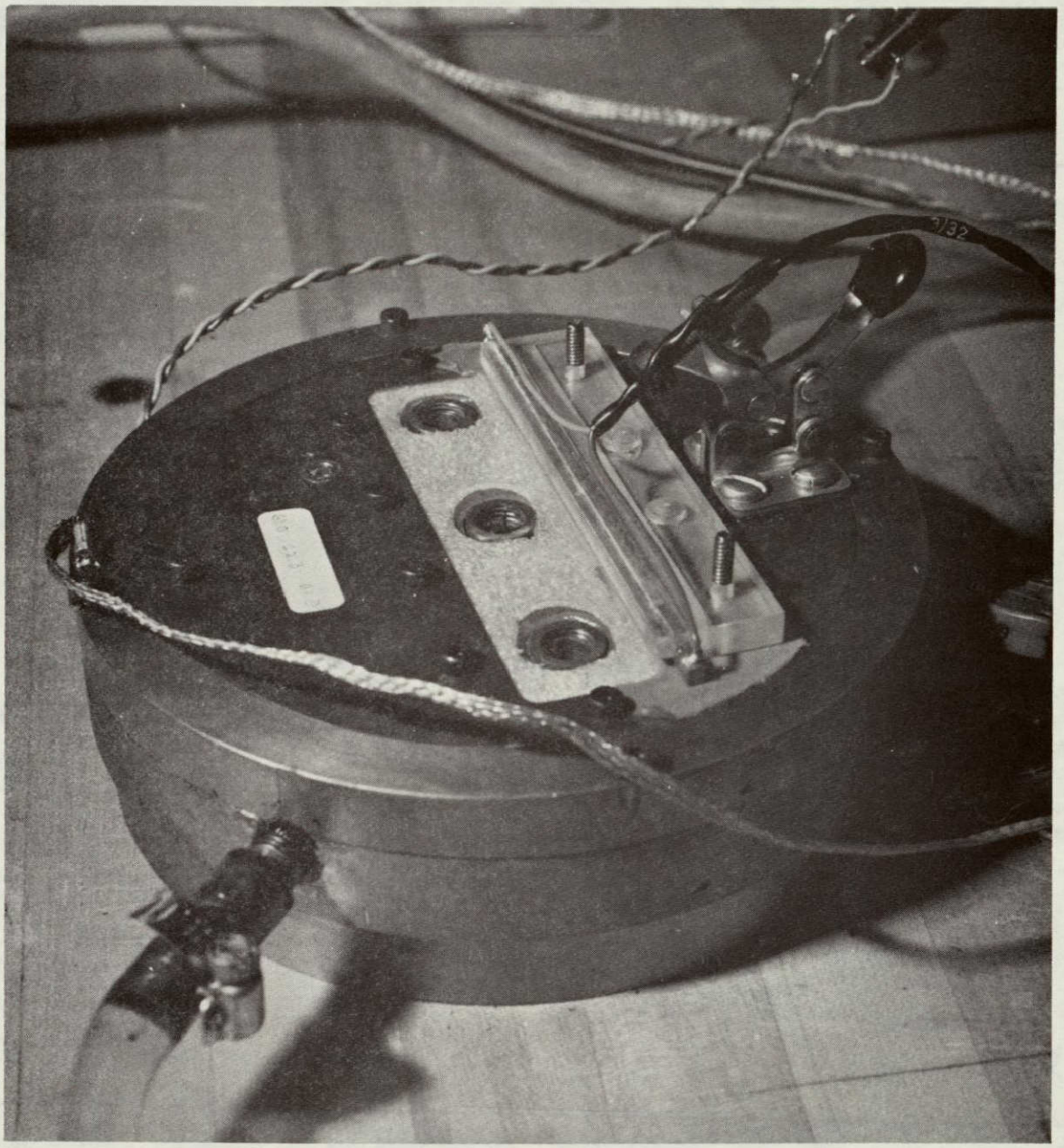

Figure 2.3 Type F Cell Electrical Measurement Jig

thermocouple/voltage probe. It was found that because of the irregular thickness of the F-cell material (EFG-material) and the roughness of the solder metalization, the vacuum hold-down allowed considerable leakage of air across the back of the cells. This air flow, which varied from cell to cell, caused the cell temperatures during measurement to be different from the desired 28°C. Previously, when effects of this sort had occurred, the water bath temperature had been adjusted to bring the cell temperature within the measurement condition limit of 28°C $\pm$ 0.5°C. In the case of the F-cells the temperature excursions were too large to permit temperature correction within a reasonable time. Figure 2.4 shows the distribution of measurement temperatures for the F-cell test population for a constant water bath temperature of 26°C. Since the measurement temperature differs from 28°C the absolute accuracy of the measured parameters will suffer. However, it was hoped that with a constant water bath temperature each cell would achieve the same equilibrium temperature each time it was measured and consequently measurement repeatability would not suffer. This did not prove to be correct, presumably because of slight differences in the placement of cells in the test jig. Consequently it was necessary to perform a software correction in the computer to correct for temperature differences.

In order to obtain the correction factors for F-cells, 5 cells were measured with a constant water cooling temperature of 20°C, 26°C, and 40°C. Two of the 5 cells were chosen to show large leakage, two to show small leakage, and one was the standard cell, which showed average leakage. The results are shown for 3 of the cells in the curves of Figures 2.5, 2.6, and 2.7. Only 3 cells are indicated in the curves to avoid confusion, but the slopes shown are based on an

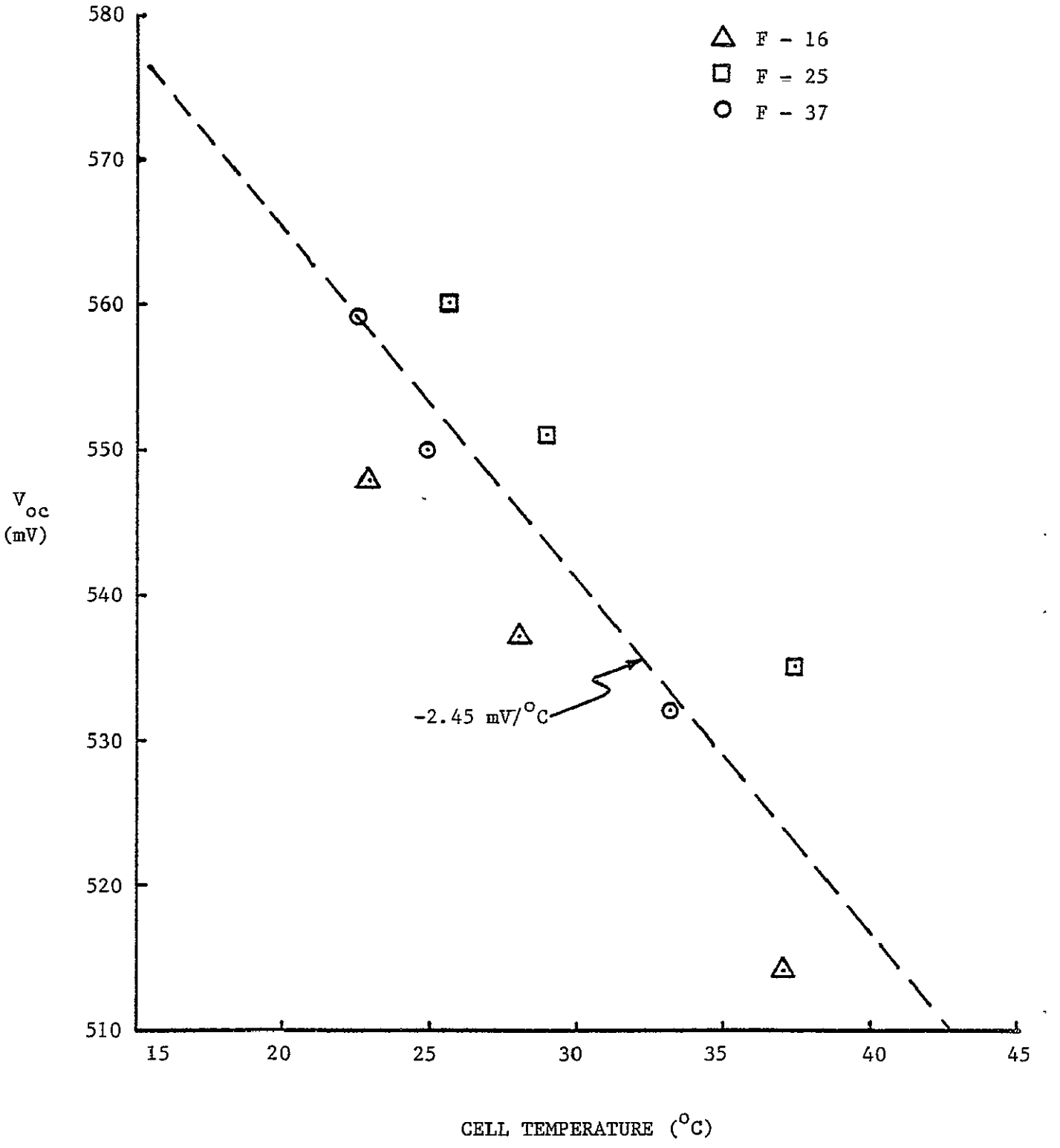

Figure 2.5. $-V_{oc}$ vs. T for F-Cells Showing Average Slope.

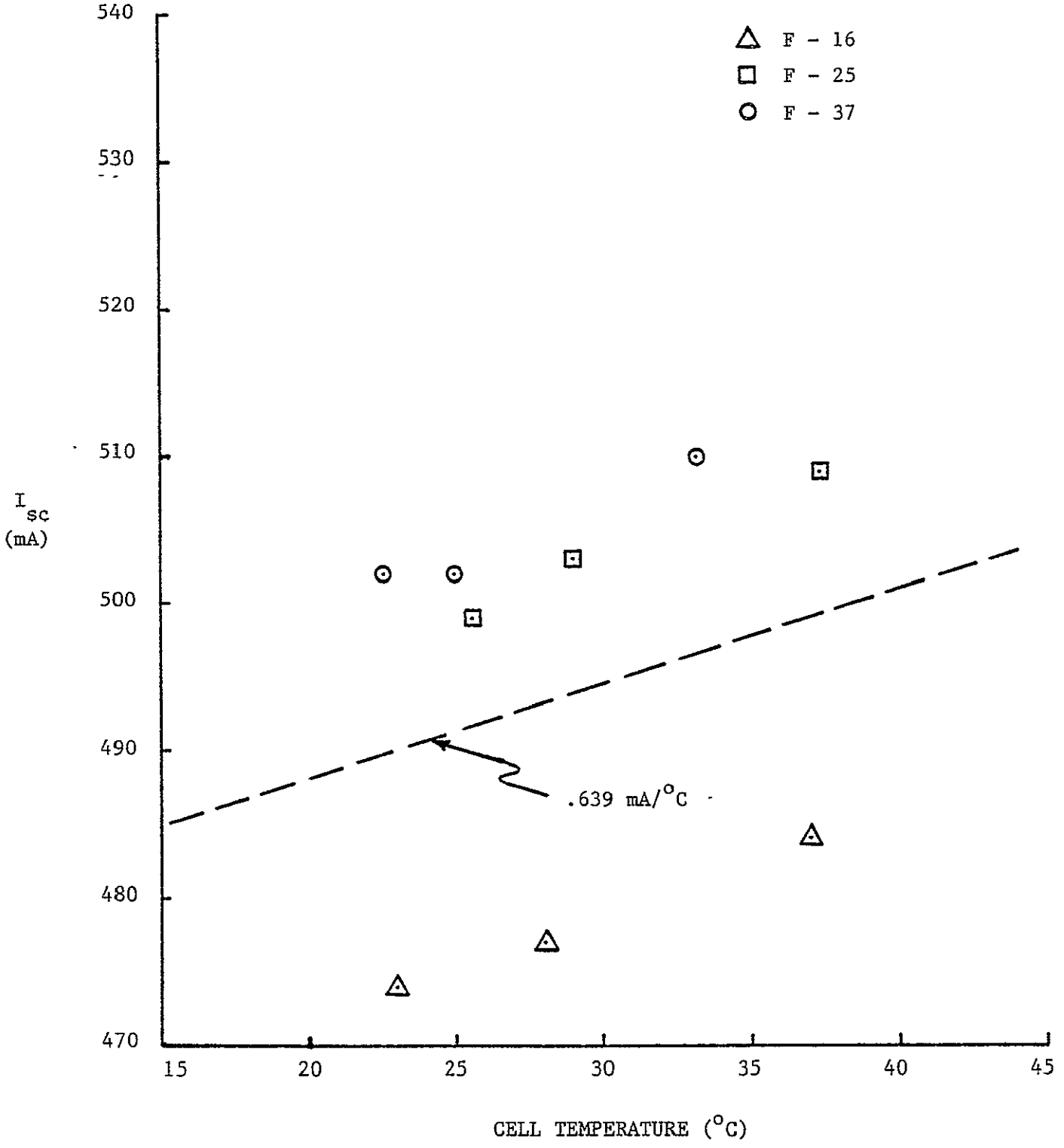

Figure 2.6. I_{sc} vs. T for F-Cells Showing Average Slope.

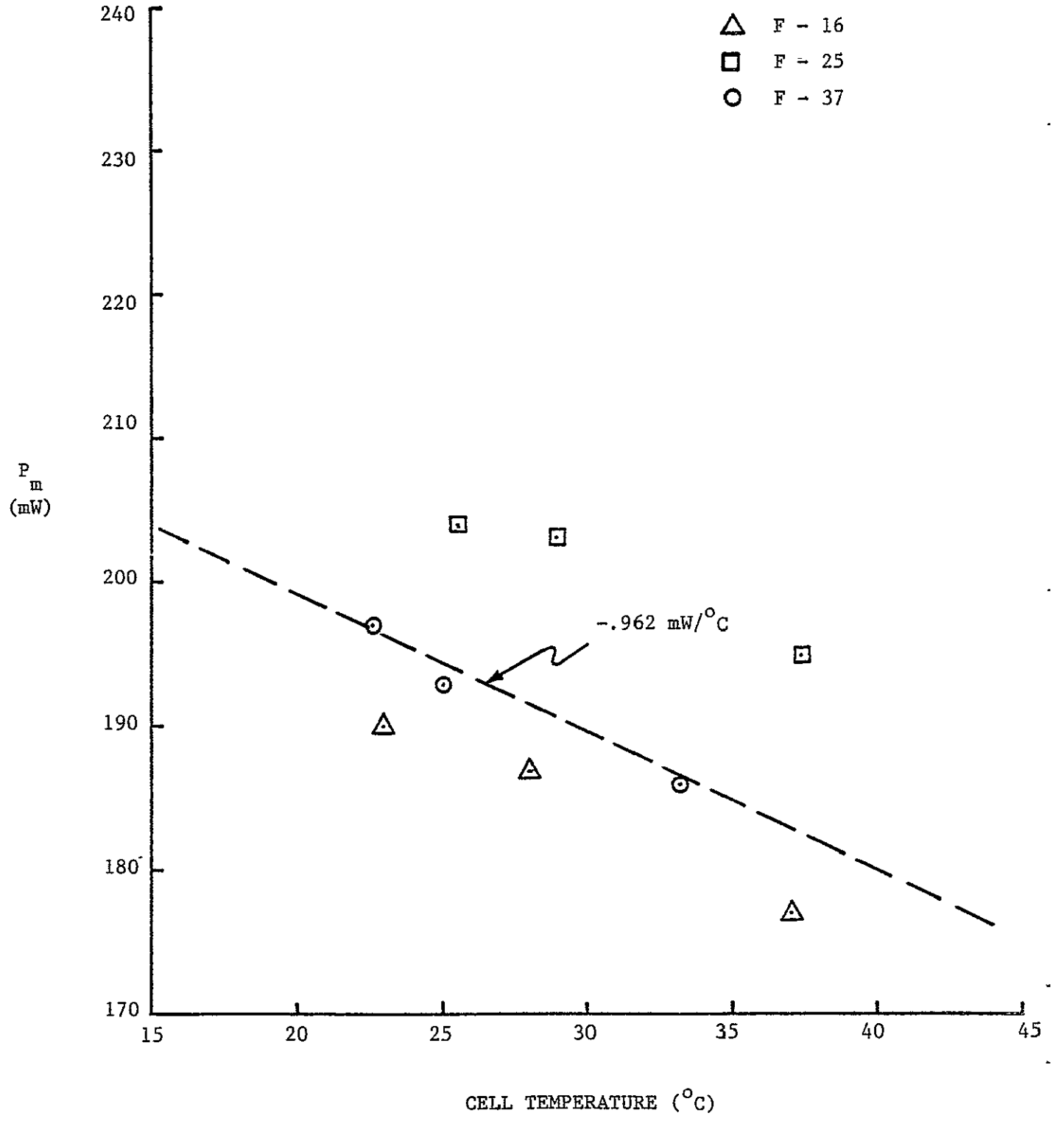

Figure 2.7. P_m vs. T for F-Cells Showing Average Slope.

average of least squares fitting to data of all 5 cells. The correction factors for F-cells are therefore,

$$V_{oc}\ (28^{o}) = 2.45 \times 10^{-3}\ (T - 28) + V_{oc}\ (T)$$

$$I_{sc}\ (28^{o}) = -6.39 \times 10^{-4}\ (T - 28) + I_{sc}\ (T)$$

$$P_{m}\ (28^{o}) = 9.62 \times 10^{-4}\ (T - 28) + P_{m}\ (T)$$

where T is the temperature of the cell during measurement, expressed in ^{o}C, V_{oc} is in volts, I_{sc} is in amperes, and P_{m} in watts.

It can be noted from the scatter of the points that even though these factors are used to relate measurements made at any temperature back to the common temperature of 28°C the procedure is not perfect and does introduce an extra amount of error. In order to minimize this the standard cell was always used at 28°C when adjusting the lamp intensity to avoid compounding the error. It was found to be practical to adjust the water bath temperature for the reference cell once or twice a day.

Built into each jig was a photodiode (Motorola MRD-510) which was used to continuously monitor light intensity. The light intensity was originally set as discussed in earlier reports (see Second Quarterly Report, August 1, 1978, p. 12) using a reference cell and a standard cell. Since reference cells were not supplied with any of the new cell types, the cell type B reference cell was arbitrarily used for all. One cell from each of the three new test populations was set aside and designated as a standard cell. It was measured prior to measuring any group of cells and the data served as a check on the system's calibration. The photodiode was monitored between measurements, and if changes were observed the standard cell was remeasured. This technique avoided any problem of lamp drift. The photodiode, being in reality a miniature solar cell is itself a function of temperature. Its output

was made insensitive to temperature by heat sinking to the jig (constant temperature water bath) and by proper choice of the diode load resistor value.

The F-cell manufacturer supplied test data with each cell and this enabled comparison with Clemson data. The manufacturer's test equipment was of the "flash" type rather than equilibrium illumination, and consequently was not subject to temperature fluctuations. Comparison of the ratio of Clemson's equilibrium value to the manufacturers' transient value is shown in Table 2.1.

PARAMETER	MEAN	STD DEV
V_{oc}	1.001	.00450
I_{sc}	.915	.0166
P_m	.926	.0403

Table 2.1. Clemson F-cell Data Normalized to Manufacturers' Values.

It can be seen that V_{oc} values are equal for the two measurement techniques, but that I_{sc} and P_m are lower by Clemson's method. It was experimentally determined that all three values could be closely matched by the Clemson equipment provided the light intensity was raised (increasing I_{sc} and V_{oc}) and the cell temperature simultaneously raised (lowering V_{oc} to its original value). Since the cells were not cooled by the manufacturer during test it seems reasonable that they could run slightly warmer and since a calibrated reference cell was not available at either location the two light intensities could also be slightly different. Both measurement equipments used ELH solar simulators. The absolute differences, however, are immaterial since in this program the primary concern is with repeatability and not with absolute accuracy.

Type G cells presented a different jig design problem since they were received from the manufacturer without suitable test tabs. A Kapton® coated copper sheet had been soldered to the metalized contact pattern at 6 points, around the periphery of the cell, but could not be used for electrical connection. The copper sheet was therefore removed by cutting (no heat or force was used) and electrical test connections were made using probes rather than solder connections. The G cell test jig is shown in Figure 2.8. Since in the manufacturing process the cell had been solder dipped with subsequent reflow the back side was generally irregular except in the center where the solder coating was relatively smooth (see Figure 2.9). Consequently, in the electrical measurement jig design the vacuum hold down was restricted to this smooth central region, but the cell periphery was allowed to rest on the jig as well for additional heat removal. Temperature was monitored by means of the central thermocouple/voltage probe. As in the case of the F cells, it was not practical to measure all cells at $28 \pm 0.5^{o}C$ and it was necessary to perform a software correction to transform the data to $28^{o}C$. Figures 2.10, 2.11, and 2.12 show the variation of V_{oc}, I_{sc}, and P_m with temperature for 3 of the 5 G cells measured at cooling water temperatures of $14.5^{o}C$, $23.0^{o}C$, and $36.0^{o}C$. The correction factors, using least squares curve fitting of all 5 cells were determined to be

$$V_{oc}\ (28^{o}) = 2.16 \times 10^{-3}\ (T - 28) + V_{oc}\ (T)$$

$$I_{sc}\ (28^{o}) = -5.37 \times 10^{-4}\ (T - 28) + I_{sc}\ (T)$$

$$P_m\ (28^{o}) = 2.92 \times 10^{-3}\ (T - 28) + P_m\ (T)$$

where T is in ^{o}C, V_{oc} in volts, I_{sc} in amperes, and P_m in watts. A comparison of these correction factors with those for F cells

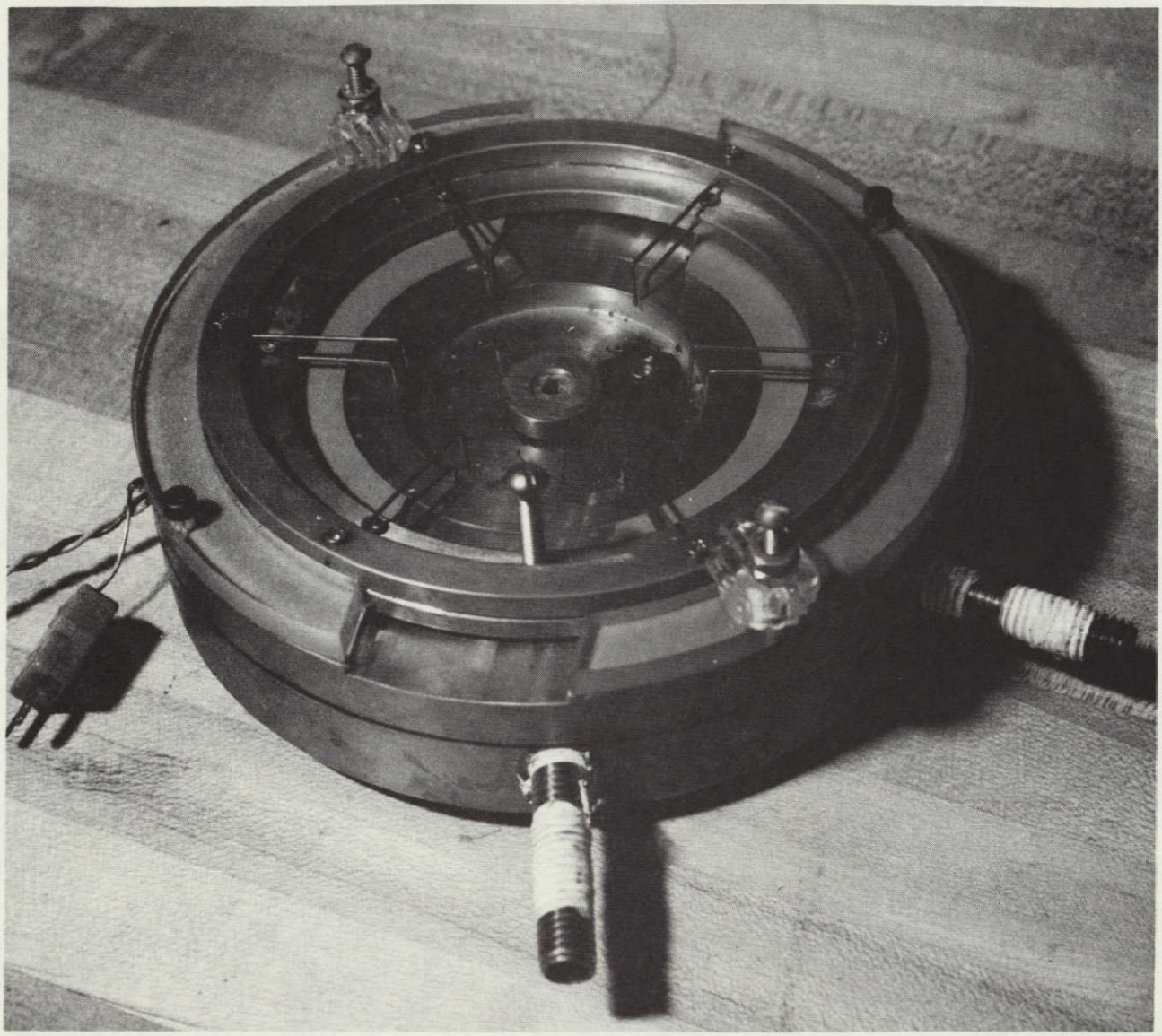

Figure 2.8 Type G Cell Electrical Measurement Jig

Figure 2.9 Back Side of Typical Type G Cell Showing Solder Irregularities

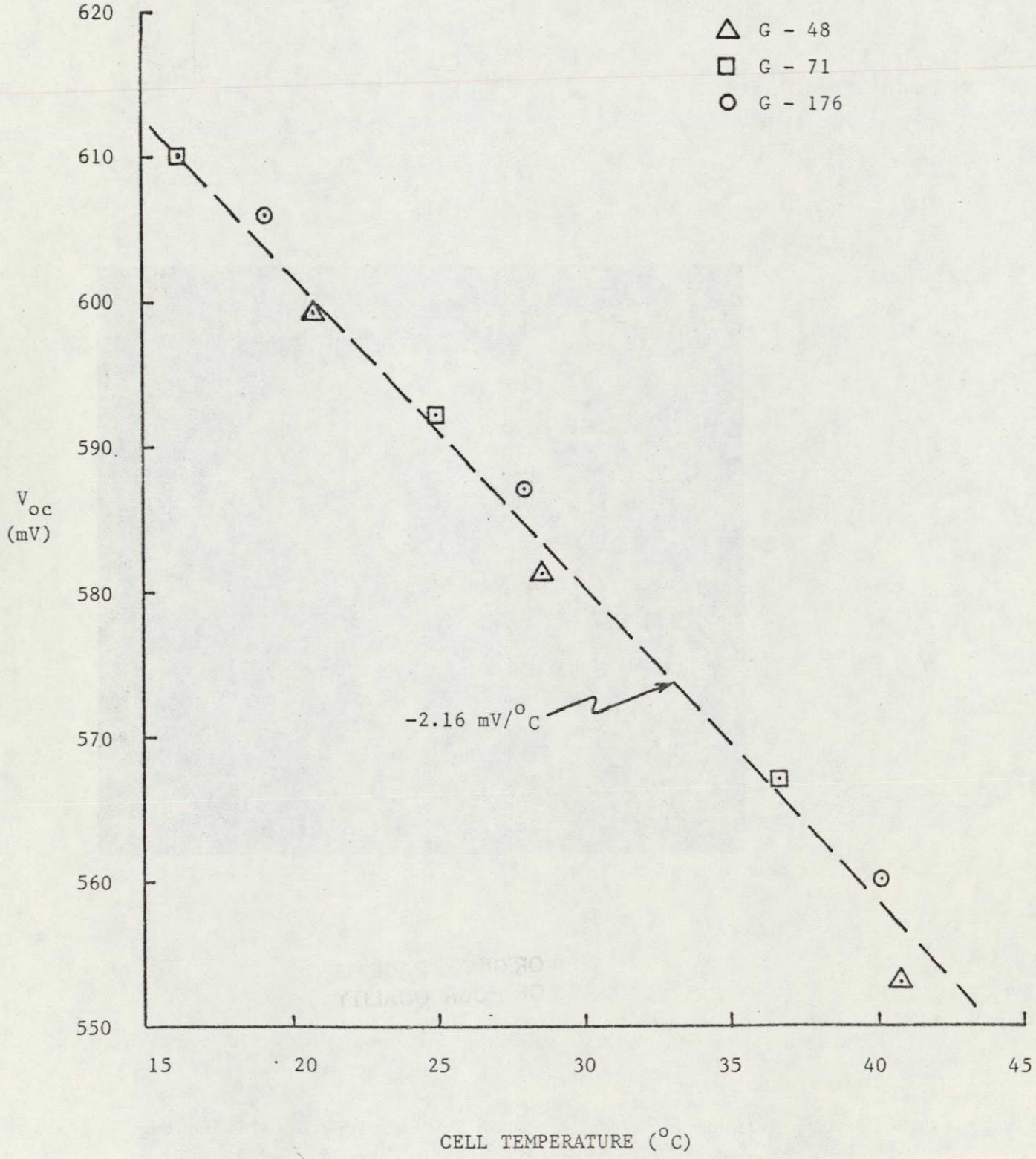

Figure 2.10. V_{oc} vs. T for G-Cells Showing Average Slope.

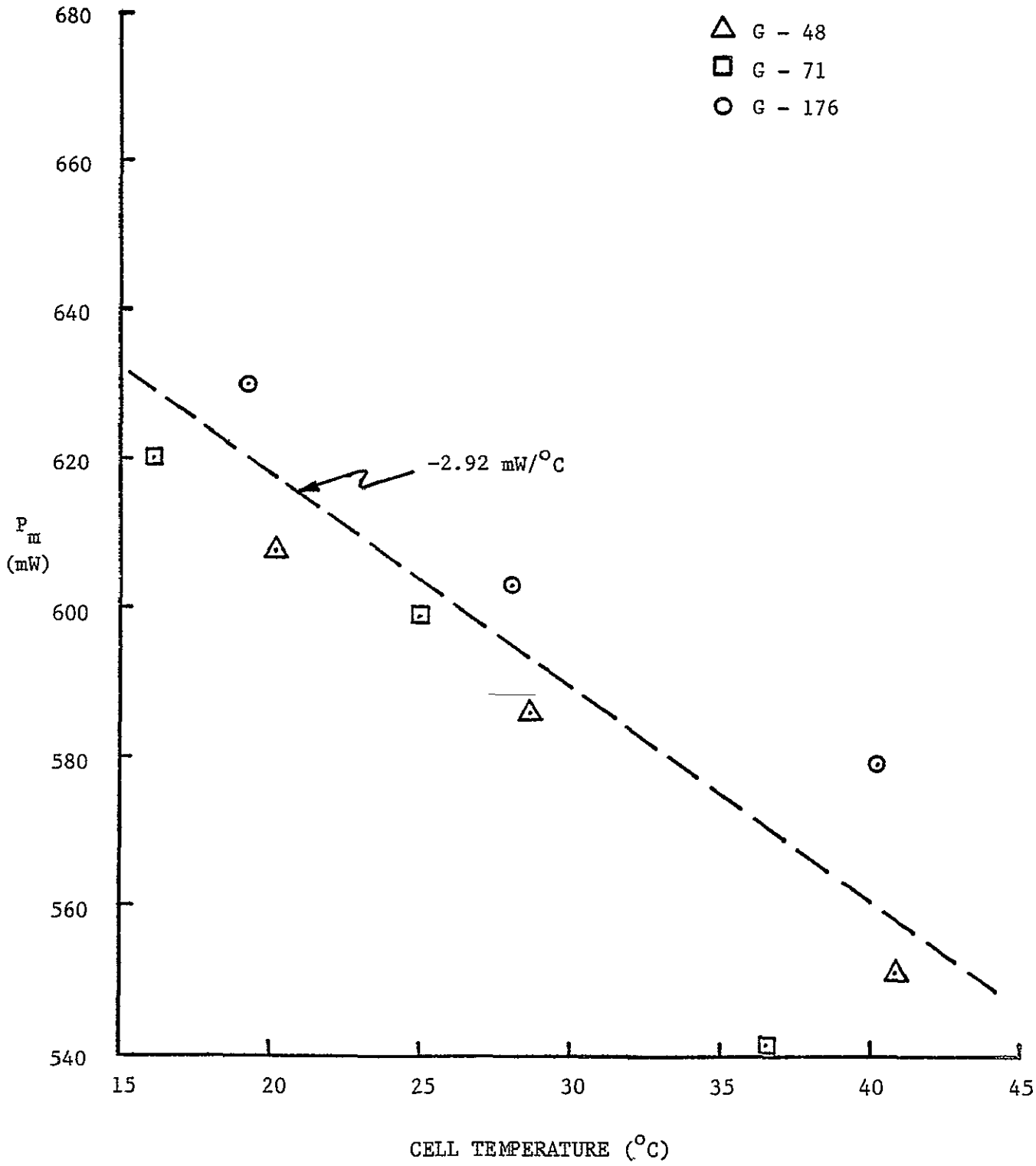

Figure 2.12. P_m vs. T for G-Cells Showing Average Slope.

indicates that the variation of V_{oc} and I_{sc} with temperature is approximately the same for the two cell types. The variation of P_m with temperature, on the other hand, is three times greater for type G cells than for type F cells. The reason for this effect is not known, but the two cell types use silicon produced by different growth mechanisms -- EFG for F cells and Czochalski for G cells. The more perfect Czochalski material shows a 40% greater absolute efficiency, but at the same time a more rapid fall off with increasing temperature, than the less perfect EFG material.

Contact to the top surface metalization of the G cells is via 6 pairs of voltage and current probes. All voltage probes were connected together as were all current probes, but the two sets were insulated from each other and separate connections brought out. The current probes were located closest to the outside of the cell. The probes could be easily and quickly aligned by eye and the cells were placed in the jig the same way each time using the flat for orientation. Reproducibility was excellent. A photodiode was incorporated in the G cell test jig as in the F cell jig. During testing of a cell it was covered, but was used to monitor lamp intensity between tests.

H cells were not received for testing during the quarter and a description of the measurement jig and temperature correction factors for this cell type will be given in the next quarterly report.

It is evident that uncorrectable temperature variations from cell to cell limit the accuracy and reproducibility that can be obtained from equilibrium-type measurement equipment. For this reason consideration was given during the quarter to design of a microprocessor based tester which would be capable of measuring V_{oc}, I_{sc}, V_m,

I_m, and P_m within 1 second. Using an electromechanical shutter, readings would be taken without heating the cell. In order to obtain sufficient resolution it is necessary to use 12-bit data in connection with a programmable power supply. Consideration was given to the choice of a microprocessor which would be suitable for this application. Possibilities were the Intel 8086, Intel 8080, Harris 6100, and Motorola 6800. A final decision has not been reached, but the proper choice appears to be between the 8080 and 6100 with the 6100 having a slight edge.

2.2 Stress Testing

2.2.1 Stress Testing Progress

The stress test schedule for the second program year was arrived at after consideration of the results of earlier testing (see First Annual Report, JPL contract 954929, May 1979) and in the light of time and manpower limitations. The schedule is shown in Table 2.2. The 165°C forward bias-temperature test used previously was excluded partially because the temperature is dangerously close to the 170°C - 175°C solder melting point. The power cycle test used previously was excluded because it produced minimal effects on the four cell types investigated in the first program year. Unbiased temperature-humidity tests were added in an effort to determine the effect of bias, if any, on temperature-humidity induced degradation. Most stress test populations were reduced to what were felt to be minimum values, based on the experience of the first year, in order to conserve manpower and thus enable additional interpretation of results.

During the reporting period the first stress test period was completed for type F and G cells for the 75°C and 150°C B-T

Stress Test	Cell Quantity per Type	Projected Downtimes (hours, cycles)
Forward Bias-Temperature, 75°C	30	600, 1200, 2400
Forward Bias-Temperature, 135°C	25	700, 1200, 2400
Forward Bias-Temperature, 150°C	25	300, 600, 1200, 2400
Temperature-Humidity (Pressure Cooker)		
Forward Biased	20	20, 100, 200, 500
Unbiased	15	20, 100, 200, 500
Temperature-Humidity (85%°C/85%RH)		
Forward Biased	20	200, 500, 1000, 2000
Unbiased	15	200, 500, 1000, 2000
Thermal Cycle	15	1, 10, 20, 40
Thermal Shock	15	1, 10, 20, 40

Table 2.2. Stress Test Schedule, Second Program Year.

tests, and for type F cells only for the 135°C B-T test. In addition, both biased and unbiased type F pressure cooker lots were stressed to the first downtime. The 75°C B-T test was restarted after electrical measurement and inspection. The other B-T tests will enter the second stress period early in the next reporting period. The pressure cooker stress testing will continue, and 85°C/85%RH stress testing of type F and G cells will begin early in the next period.

2.2.2 Stress Testing Results

The prestress electrical parameters of the entire type F and type G stress test populations, with the exception of thirty cells per type intended for thermal cycle/thermal shock, were obtained. Tables 2.3 and 2.4 show mean and standard deviations of the prestress parameters. More detailed distributions of the prestress electrical parameters are given in Appendix A.

Examination of prestress and poststress electrical data for type F cells subjected to 75°C B-T stress showed that no degradation had occurred. In fact, the lot mean P_m showed a slight (1.52%) improvement. This sort of behavior was seen in the first year's work for cell types with similar metalization technology. Figure 2.13 shows the distribution of P_m for the lot, both prestress and poststress. Nothing of significance was noted in the visual inspection of the lot, poststress.

Type F cells subjected to 20 hours of pressure cooker temperature-humidity (T-H) stress testing showed slight degradations of P_m. Units which were forward biased during T-H testing showed 1.50% decrease in lot mean P_m. Units which were not biased showed 2.18% decrease in lot mean P_m. Figure 2.14 and 2.15 show the distribution

Parameter	Number	Mean	Standard Deviation
V_{oc} (V)	150	0.547	0.010
I_{sc} (A)	150	0.504	0.022
V_m (V)	150	0.444	0.011
I_m (A)	150	0.442	0.026
P_m (W)	150	0.197	0.015

Table 2.3. Mean Values and Standard Deviations of Prestress Electrical Parameters, Type F Cells.

Parameter	Number	Mean	Standard Deviation
V_{oc} (V)	151	0.589	0.004
I_{sc} (A)	151	1.341	0.023
V_m (V)	151	0.494	0.007
I_m (A)	151	1.219	0.032
P_m (W)	151	0.602	0.020

Table 2.4. Mean Values and Standard Deviations of Prestress Electrical Parameters, Type G Cells.

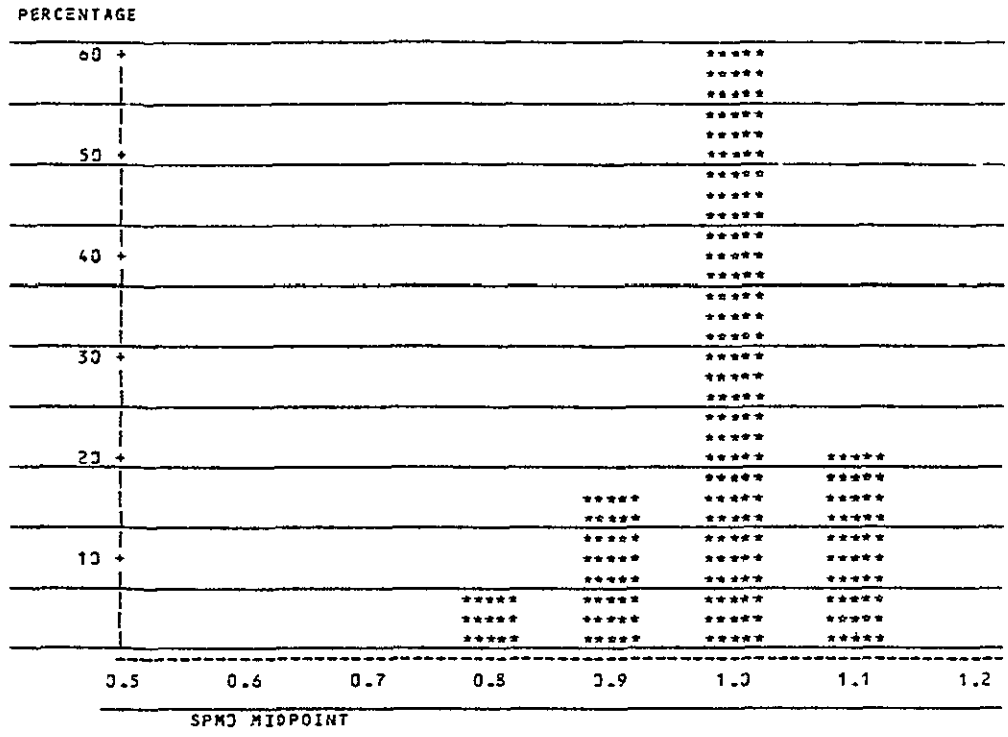

(a)

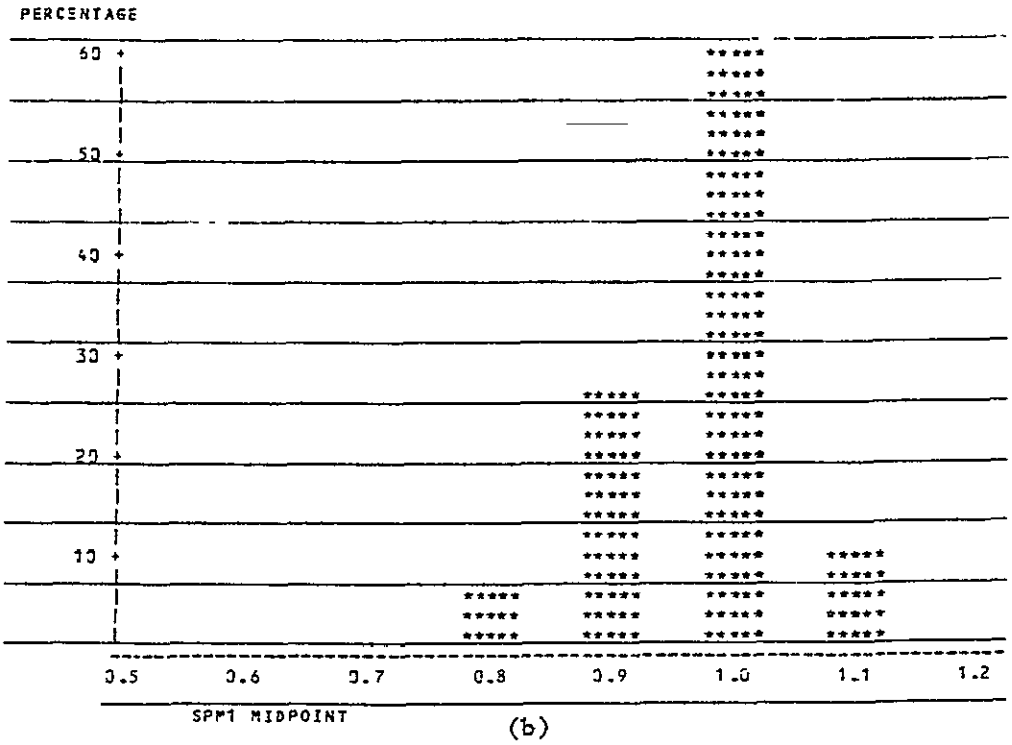

(b)

Figure 2.13. Distribution of P_m, Normalized to Prestress Lot Mean P_m, Type F Cells, 75°C B-T Stress Test. (a) Prestress, (b) Poststress, 600 Hours.

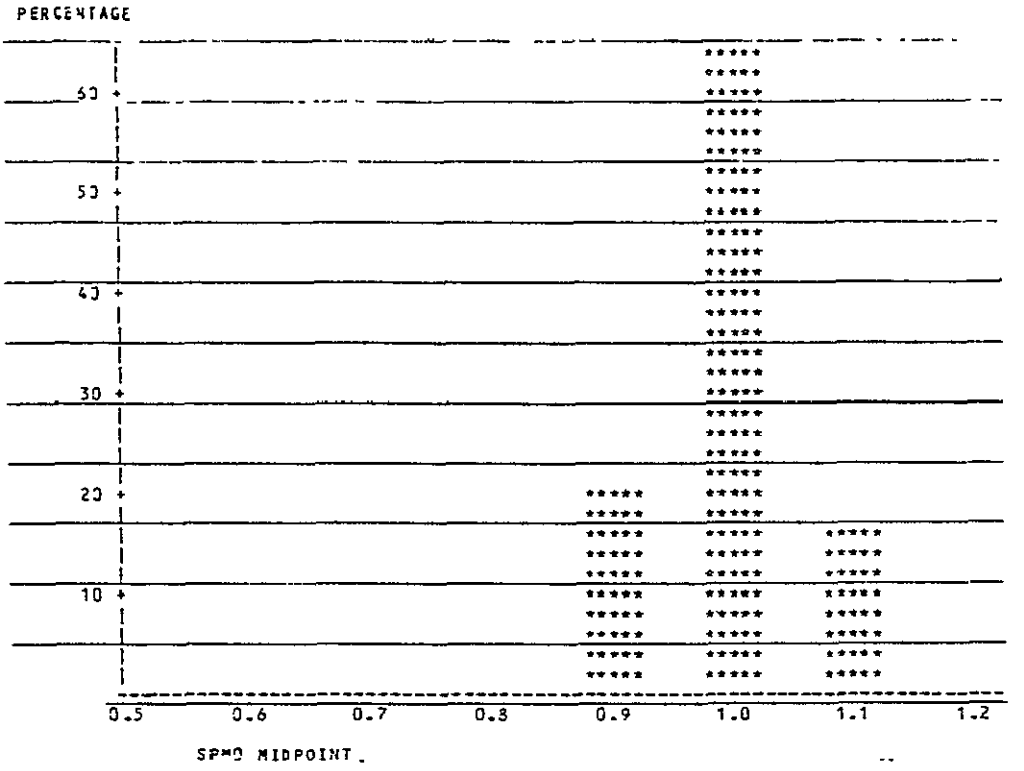

(a)

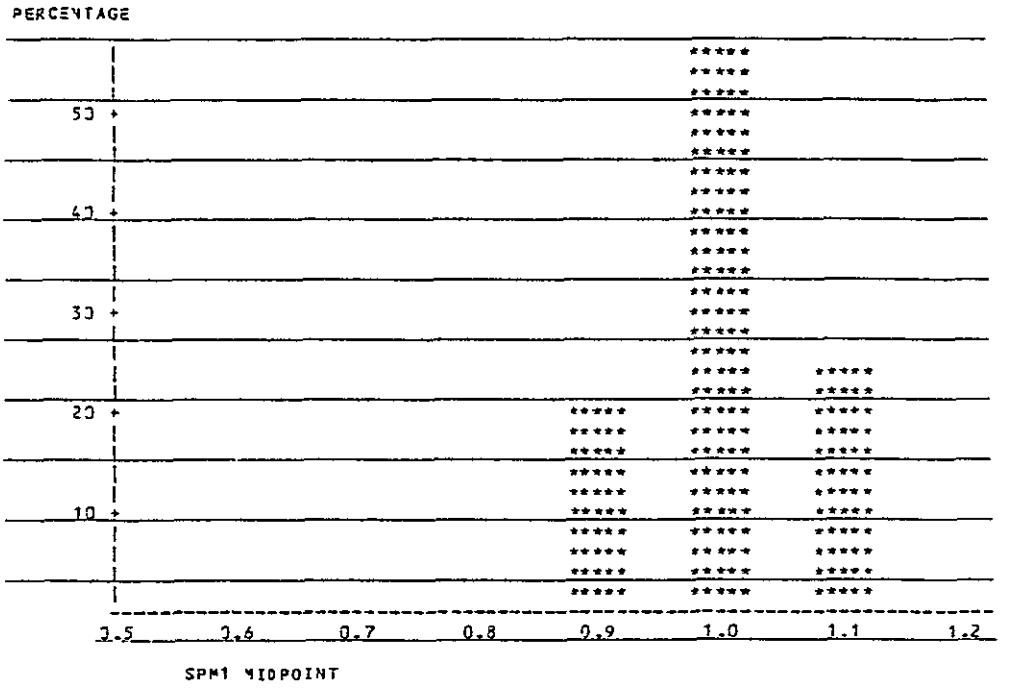

(b)

Figure 2.14. Distribution of P_m, Normalized to Prestress Lot Mean P_m, Type F Cells, Biased Pressure Cooker T-H Stress Test. (a) Prestress, (b) Poststress, 20 Hours.

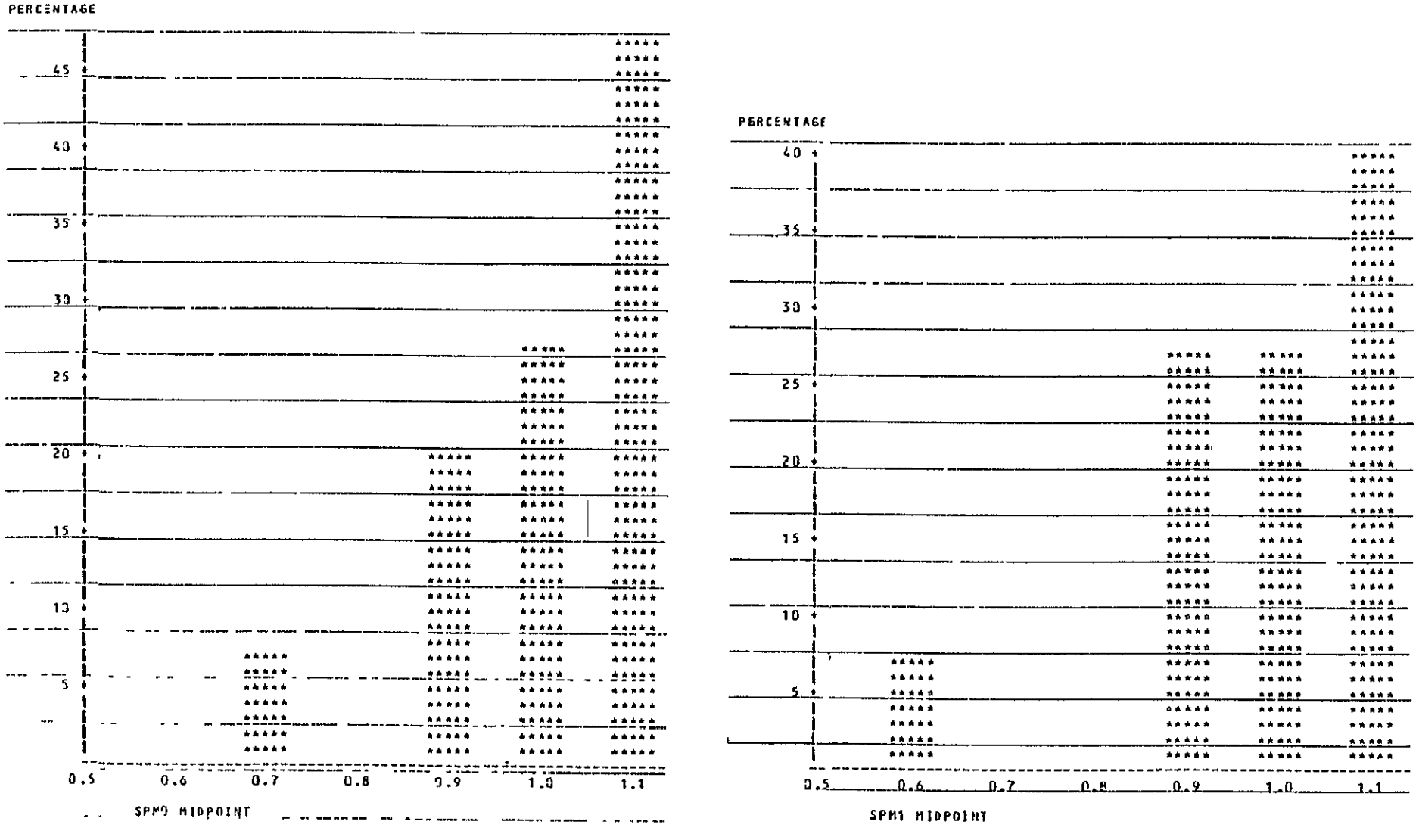

(a) (b)

Figure 2.15. Distribution of P_m, Normalized to Prestress Lot Mean P_m, Type F Cells, Unbiased Pressure Cooker T-H Stress Test. (a) Prestress, (b) Poststress, 20 Hours.

of P_m for the two lots, both prestress and poststress. The behavior observed for the unbiased units was not expected, and is thus puzzling. Even more puzzling was the discovery of large (1/8" diameter or greater) bubbles in the backside solder of the cells subjected to unbiased T-H testing. The bubbles did not appear in the bias T-H stress tested units. An interpretation of this is not yet available.

2.2.3 Stress Test Fixturing

The use of miniature alligator clips to suspend and interconnect cells in the B-T and B-T-H chambers, has many disadvantages as demonstrated by the experience with A,B,C, and E-cells during the first year of the program. In order to overcome these jigging problems a new cell test holder was developed. Specific advantages of the new design are:

1. Elimination of stress applied to cell tabs and tab attachment points.
2. Greatly reduced loading and unloading times.
3. Elimination of the need to locate shorted cells after loading.
4. Increased interconnection flexibility.
5. Increasing packing density while maintaining comparable air flow over cells.

An exploded view of the new-design cell holder is shown in Figure 2.16. Figure 2.17 shows a photograph of the test holder being loaded. The frame consists of vertical metal rods covered with insulating teflon tubing and a stablizing bottom plate. Series connection of cells is achieved through the use of convoluted beryllium-copper springs which connect the top surface lead pattern of one cell to the bottom of the overhead plate, which is in turn directly connected to

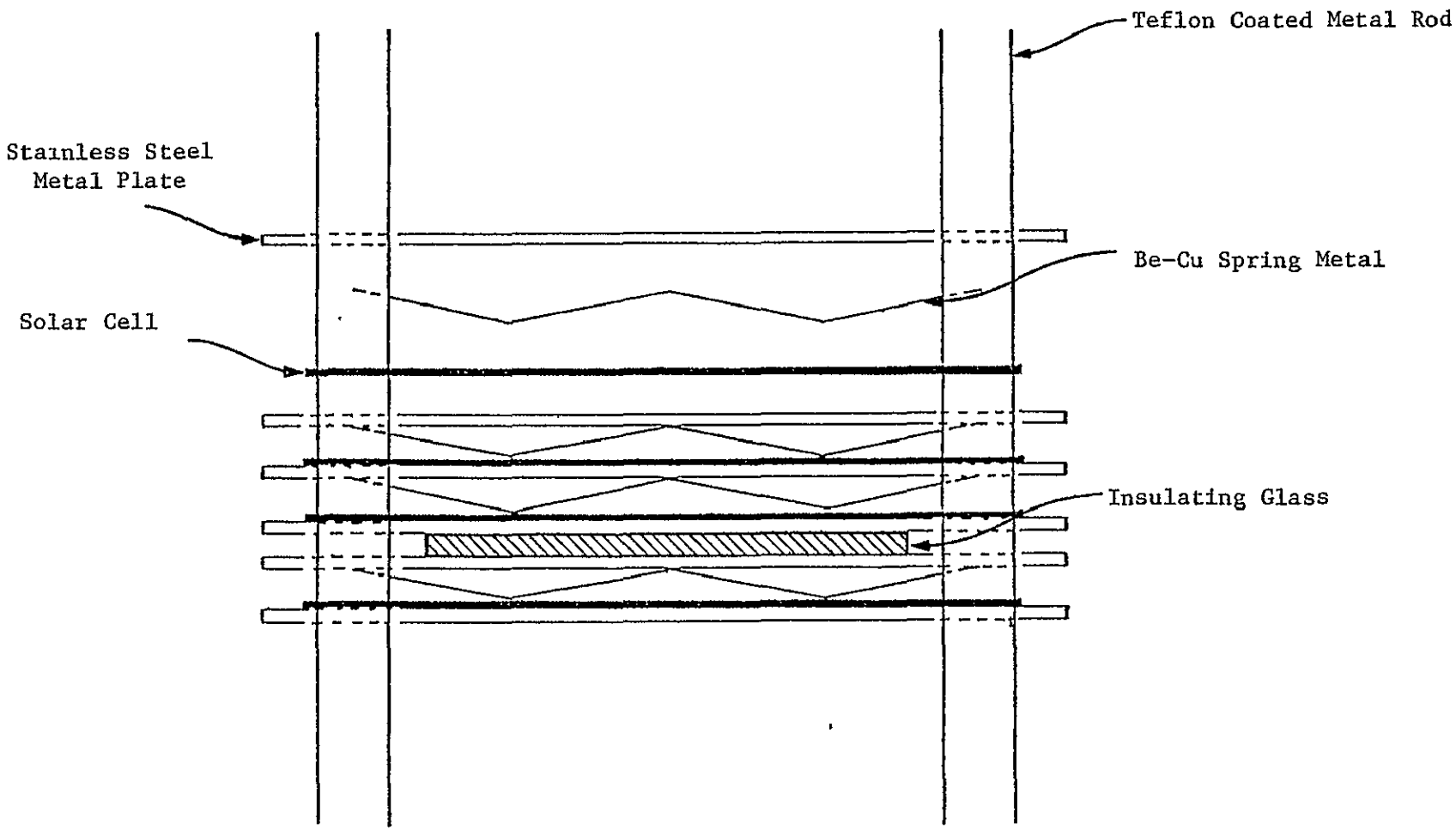

Figure 2.16. Schematic Exploded View of New-Design Stress Testing Jig.

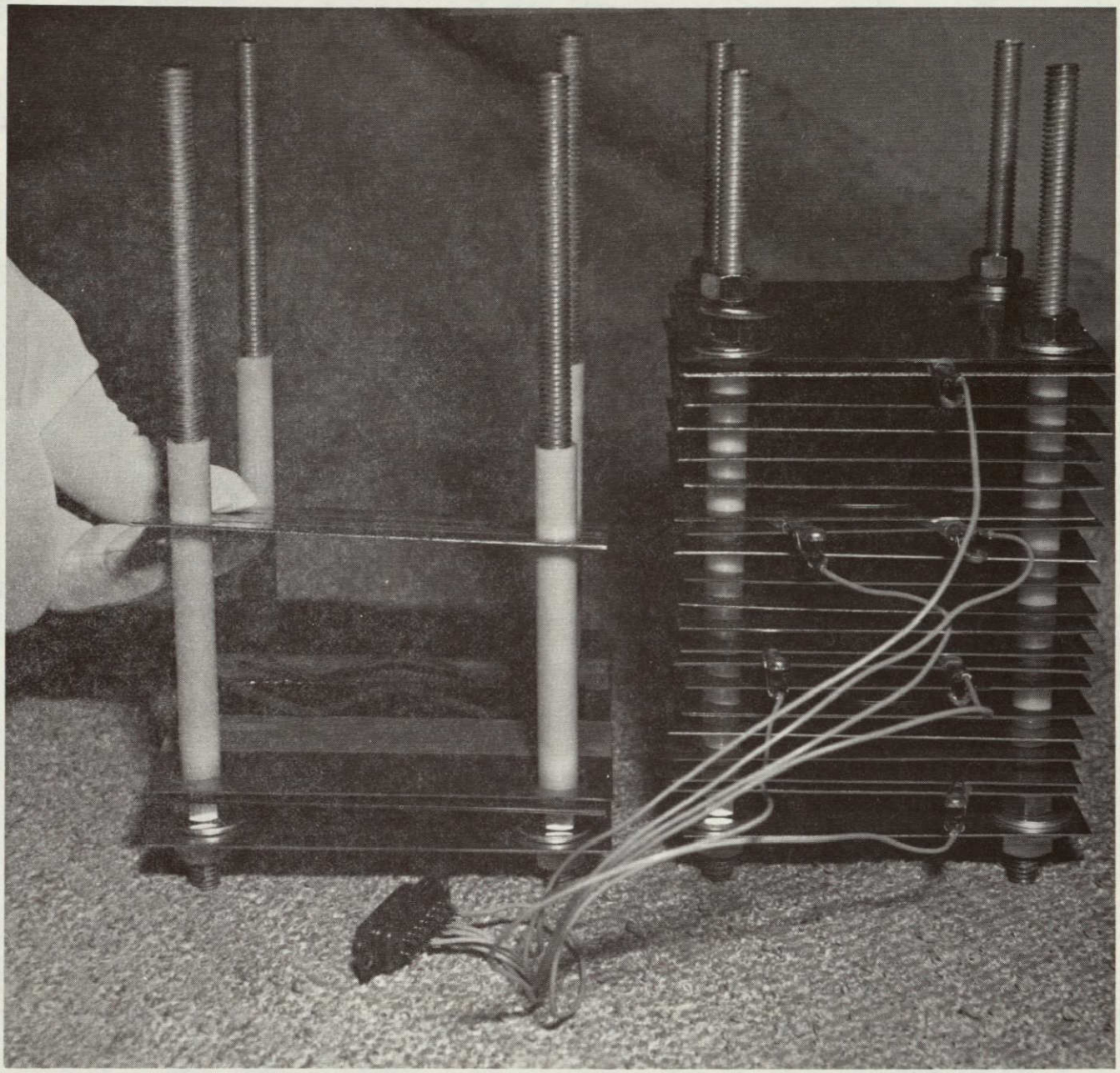

Figure 2.17 Photograph of New-Design Stress Testing Jig Being Loaded

the back of the next cell, and so on. As used in the B-T stress tests a completed "stack" consist of 3 parallel connected sets of cells; each set is in turn composed of 5 serially connected cells. Insulation of one set from the other is achieved through an insulating glass spacer between the top plate of one set and the bottom plate of the next. Additional insulation of cell leads is performed through the use of teflon adhesive tape. Tightening of the top nuts compresses the stack and ensures good electrical connection.

All jig materials were chosen for reliable performance at elevated temperatures. The spring metal was made of beryllium-copper which retains its springiness, electrical conductivity and stability to temperatures of 175°C -- well above the highest test temperature of 150°C. Preliminary tests showed tarnishing of the beryllium-copper, but this does not seem to affect the alloy's performance. The plates were made of 30 mil stainless steel to ensure good electrical conductivity, stability, and rigidity allowing each plate to support the column of plates and cells above it without bending, thus reducing the stress on the cells.

Thus far in the program no difficulities have been encountered with the new jigs and the design appears ideal for B-T stress testing. Its effectiveness in B-T-H testing will be evaluated during the next quarter.

2.3 Second Quadrant Studies

Effort was initiated on the shape of the voltage-current characteristics in the second quadrant of operation (reversed voltage). The objective of this study is to ultimately to be able to quantify

Critical to progress in the study of second quadrant phenomena is characterization of the problem. It will be necessary both to define what is to be measured, and to develop how the measurements are to be performed. Presently measurements are being made with an x-y plotter, a programmable power supply and a variable light source. This method gives a good hard copy of the data, but cause the cell to dissipate so much energy that the back of the cell reads a temperature of up to 15°C higher after the measurement. This is unacceptable for an accurate and repeatable measurement method since nearly all characteristics of the IV curve are temperature dependent. Some examples of the data obtained with the available instrumentation are presented in Figure 2.18. Transient measurements have to be taken to obtain accurate and repeatable results. This can be done with a curve tracer with a high current fixture which is currently not available at Clemson University.

In some cases the breakdown voltage is dependent on the level of illumination as shown in Figure 2.18(b). The cell enters a region of negative resistance after breakdown occurs. This can be attributed to a filamentary conductance system as is sometimes observed in power diodes or transistors. A hot spot of this type was observed once during the preliminary measurements with temperature at the hot spot well in excess of the melting temperature of the solder. This uneven temperature distribution can be observed with an infrared scanning imager, a pyricon or possibly with an infrared image converter. None of these facilities are available at the moment.

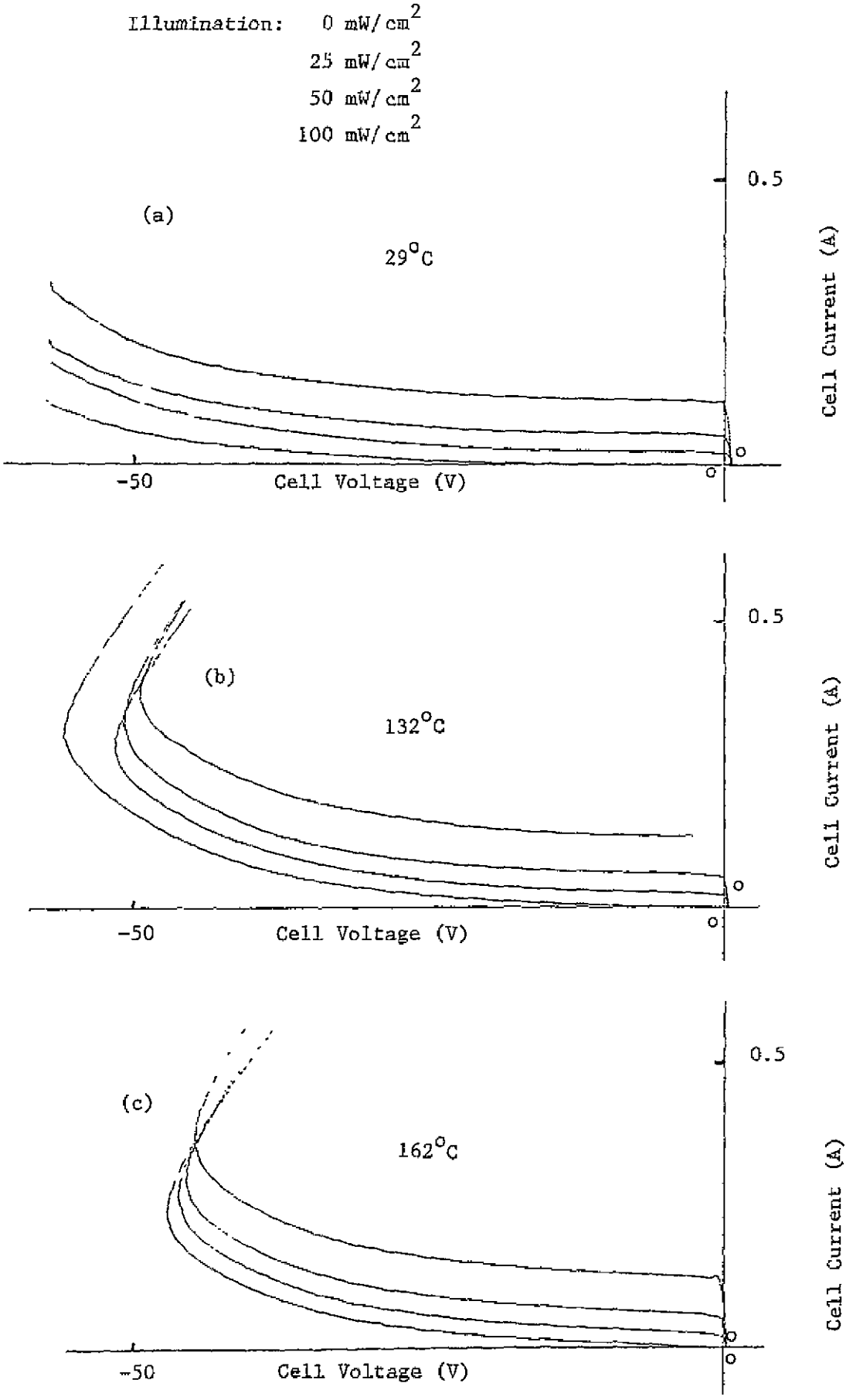

Figure 2.18. Second Quadrant Characteristics of a 2 cm x 2 cm Cell, Variable Temperature and Illumination Level.

3.0 CONCLUSIONS

At this point in the second year of the program, firm conclusions concerning degradation rates and failure mechanisms of type F, G, and H cells are not possible. However, the (incomplete) results to date indicate performance of type F cells similar to that of type B cells in the first year of effort. The new-design stress testing jig appears to have solved a major problem at least for B-T stress testing.

The electrical measurement problems encountered (e.g. non-planar cells, strange tab technology, etc.) have been handled in ways that appear to be at least near to optimum, given the instrumentation limitations which exist. Satisfactory electrical measurements are being made. The software correction for temperature variations promises acceptable results. However, measurement throughput and accuracy does suffer under present circumstances, pointing up the need for a rapid-measurement system for cells.

Review of the literature and preliminary measurements constitute the progress in the area of second quadrant effects. Experience to date bears out earlier conclusions about the need for high-current pulsed instrument action in order to carry out meaningful second quadrant measurements on terrestrial cells.

4.0 RECOMMENDATIONS

Because of the difficulties encountered with non-conventional cell structures, it is recommended that effort be devoted to developing instrumentation for a fast, automated cell measurement system.

5.0 NEW TECHNOLOGY

No reportable items of new technology have been identified during the reporting period.

6.0 REFERENCES

1. F. A. Blake and K. L. Hanson, The "Hot Spot" Failure Mode for Solar Cells, 4th IECEC, 1969 Record, pp 575-581.

2. R. M. Diamond and E. D. Steele, Solar Arrays with Integral Diodes, ICSC, Taulause, July 1970, pp 407-423.

3. P. L. Jett and J. L. Miller, Analysis of Effects of Shadowed and Open Solar Cells on Orbital Workshop Solar Cell Array Performance, 6th IECEC, 1971 Record, pp 889-900.

4. R. G. Ross, Interface Design Considerations for Terrestrial Solar Cell Modules, 12th P.S.C. 1976, pp 801-806.

APPENDIX A: Electrical Parameter Distributions of Type F and Type G Solar Cells

In this Appendix the prestress distributions of the five primary electrical parameters are shown for types F and G cells. The distributions were obtained by measurement of the parameters of 150 type F cells and 151 type G cells. These cells constitute the total stress test populations except for the cells which will be used in the thermal shock and thermal cycle tests.

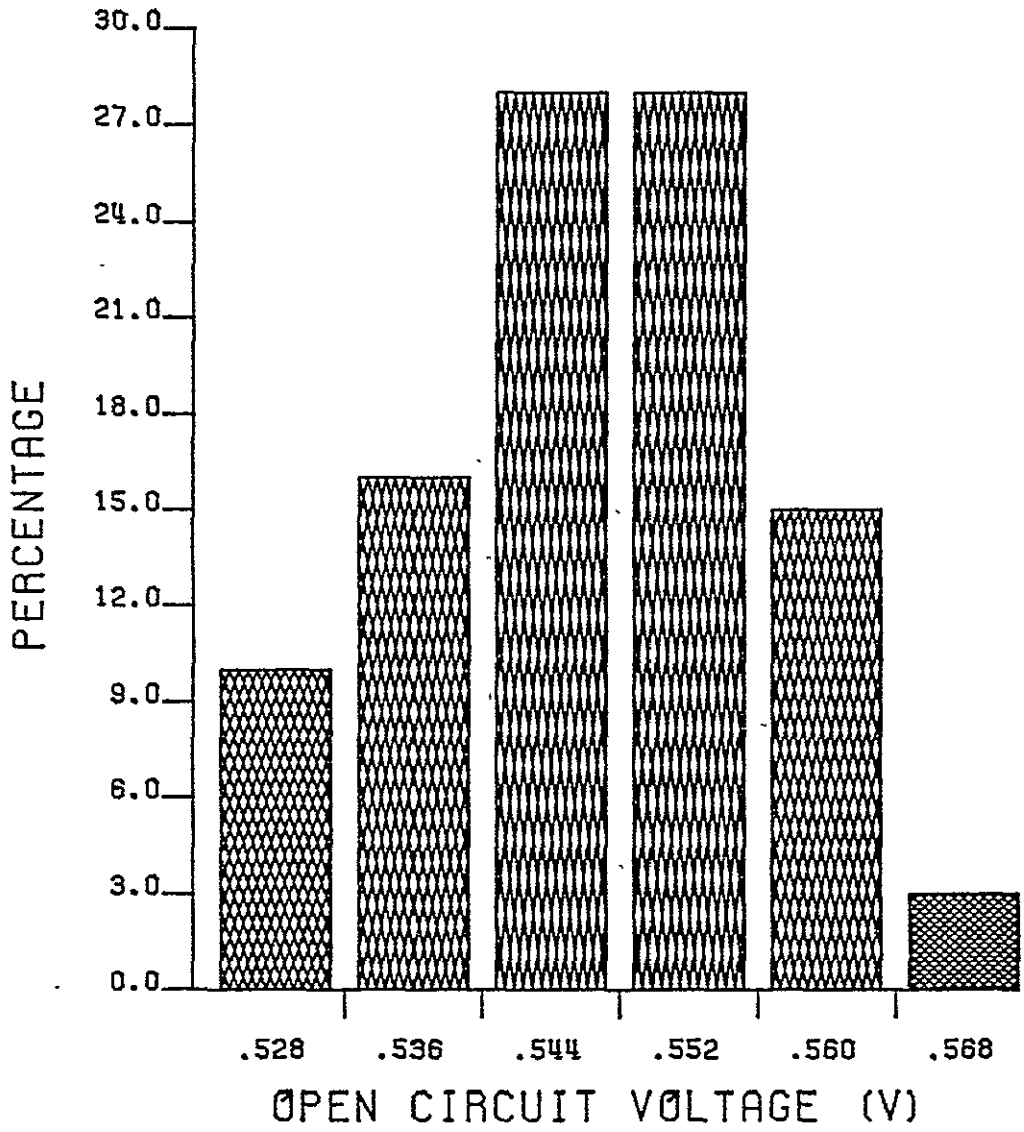

Figure A-1. Prestress Distribution of V_{oc}, Type F.

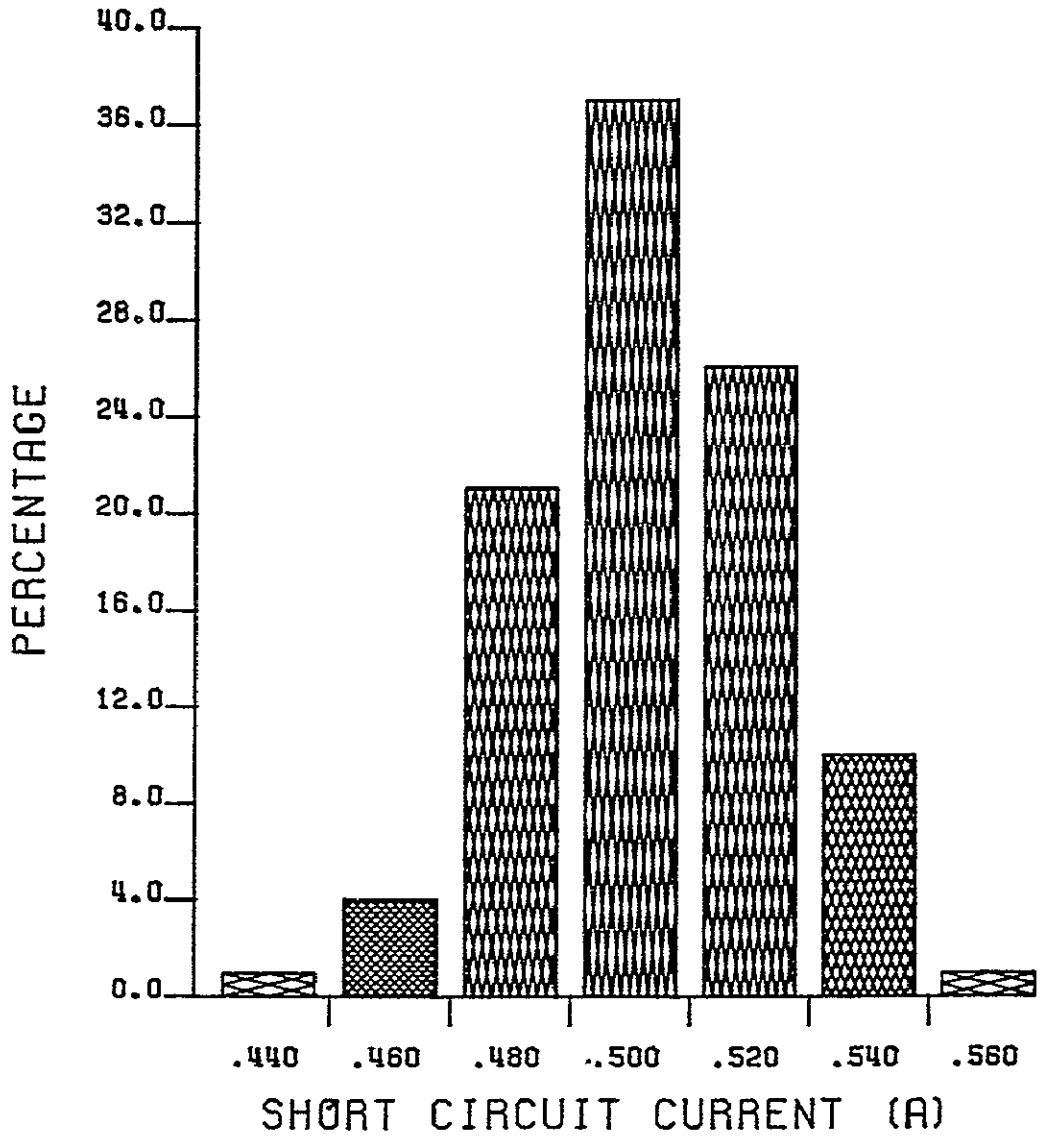

Figure A-2. Prestress Distribution of I_{sc}, Type F.

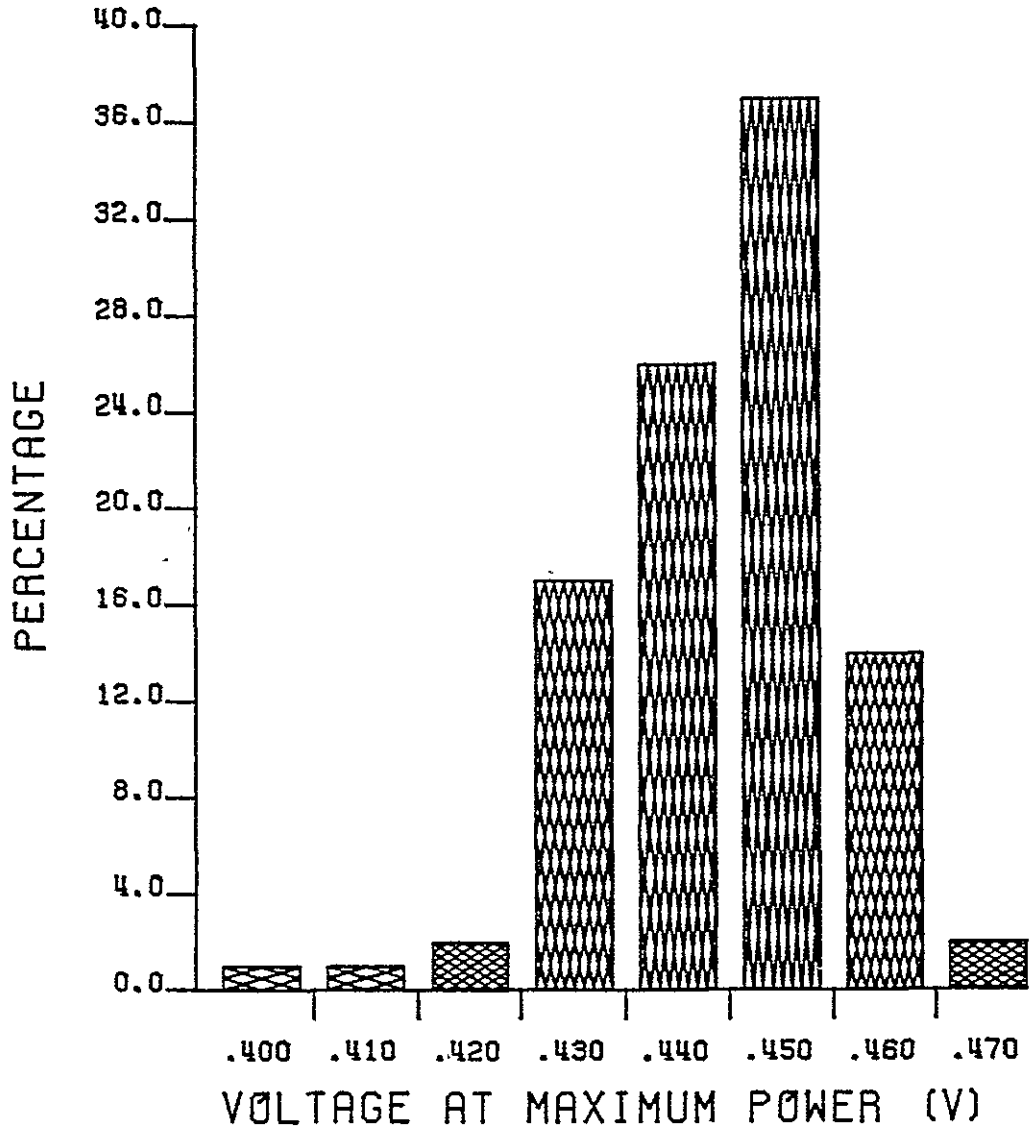

Figure A-3. Prestress Distribution of V_m, Type F.

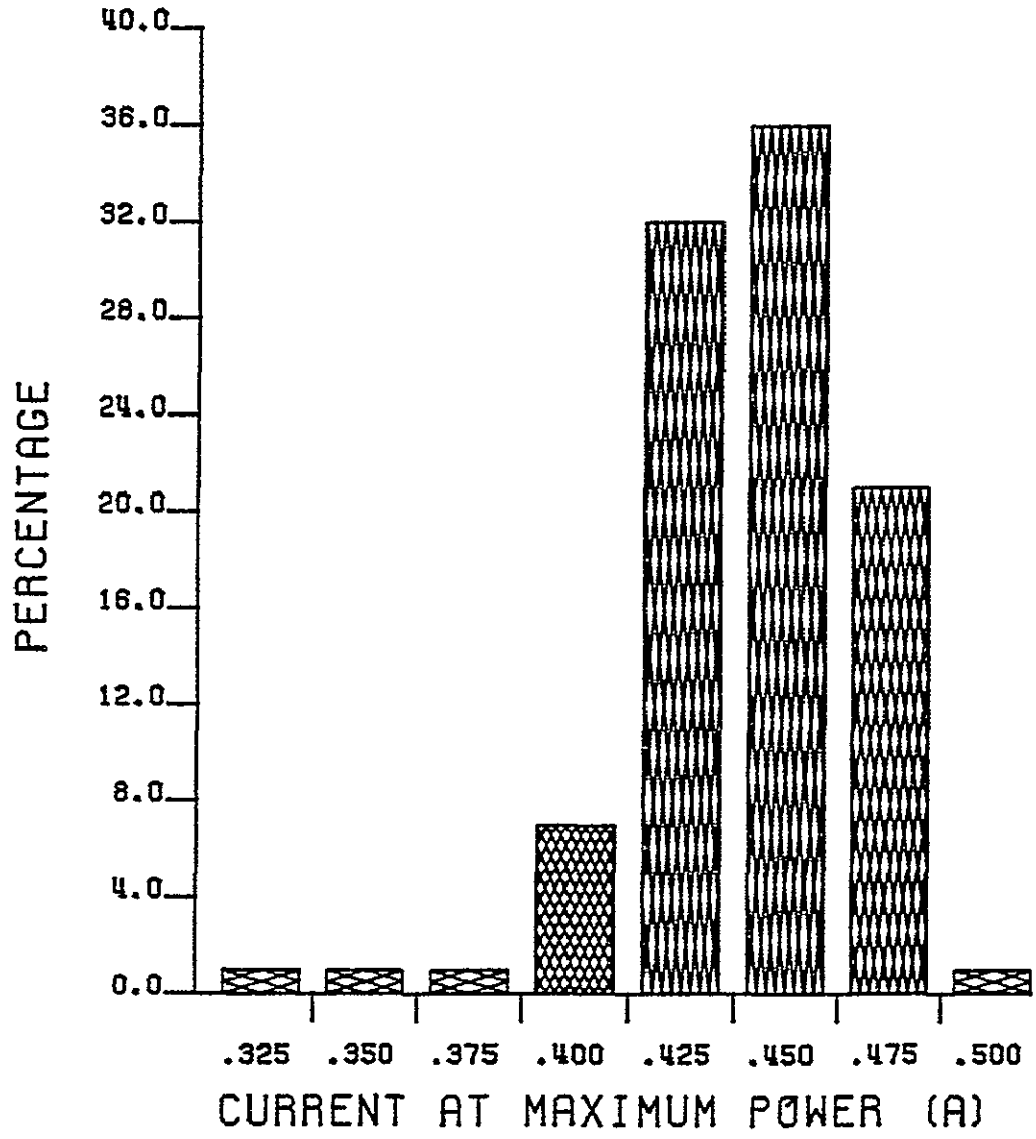

Figure A-4. Prestress Distribution of I_m, Type F.

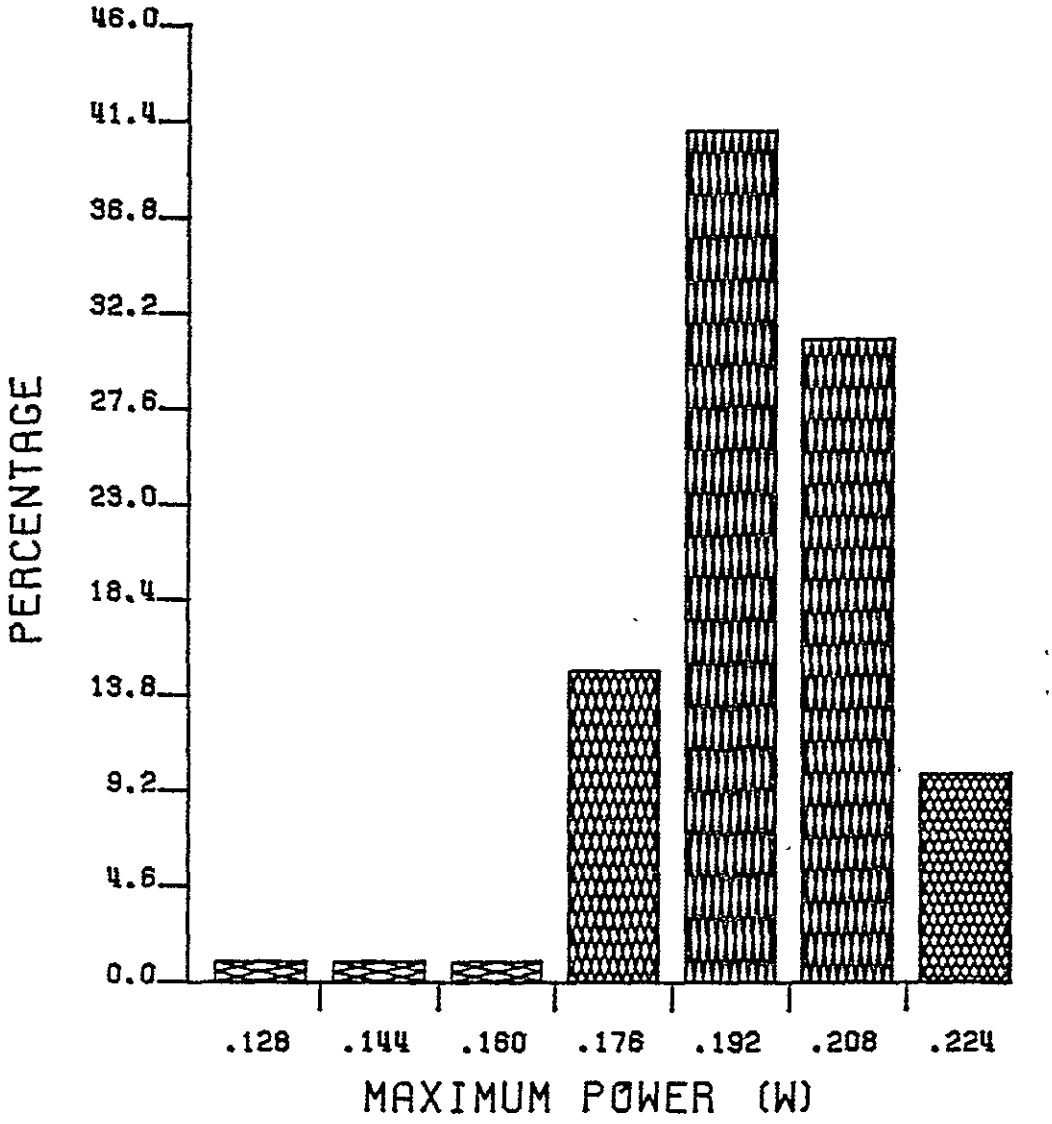

Figure A-5. Prestress Distribution of P_m, Type F.

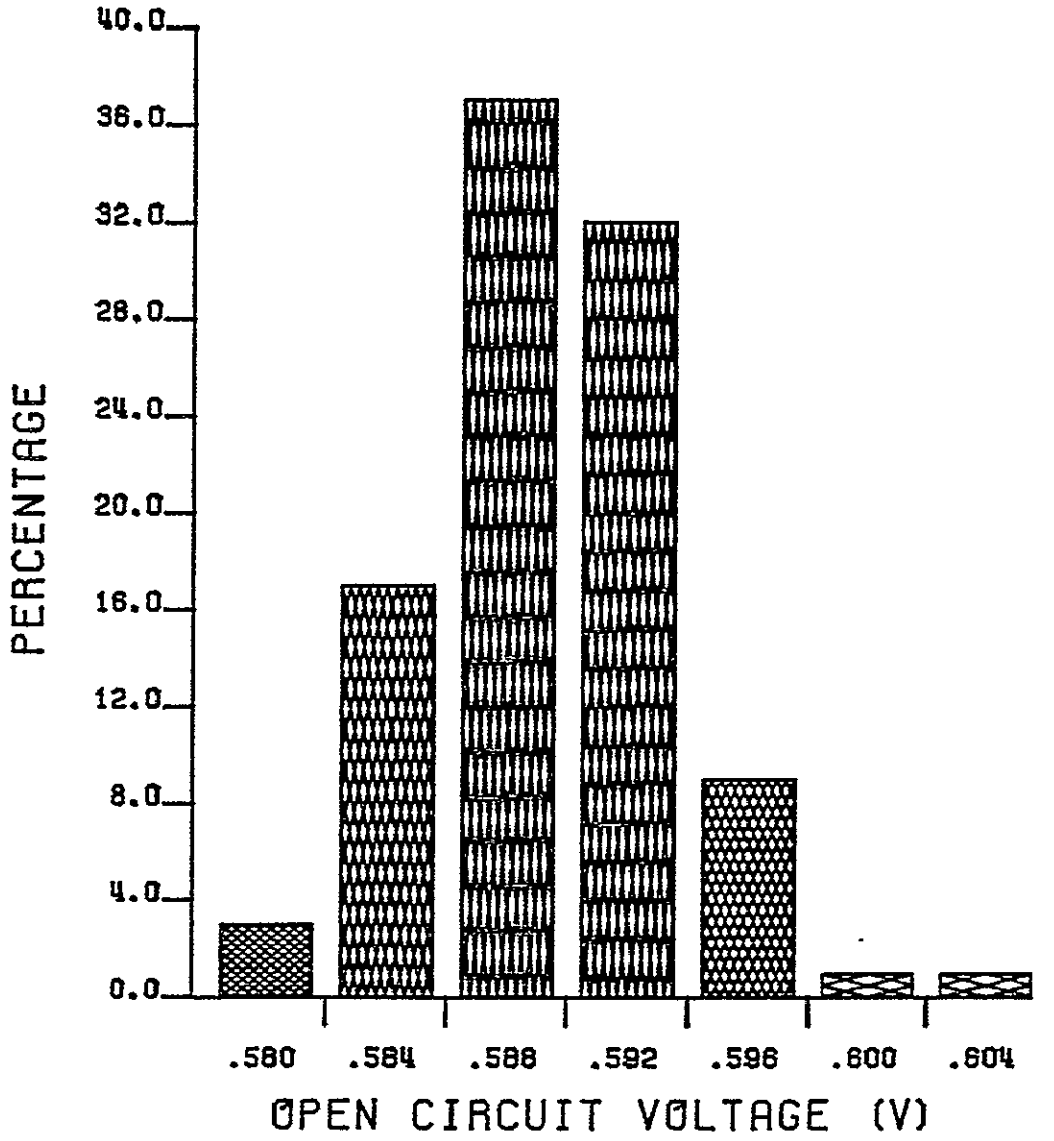

Figure A-6. Prestress Distribution of V_{oc}, Type G.

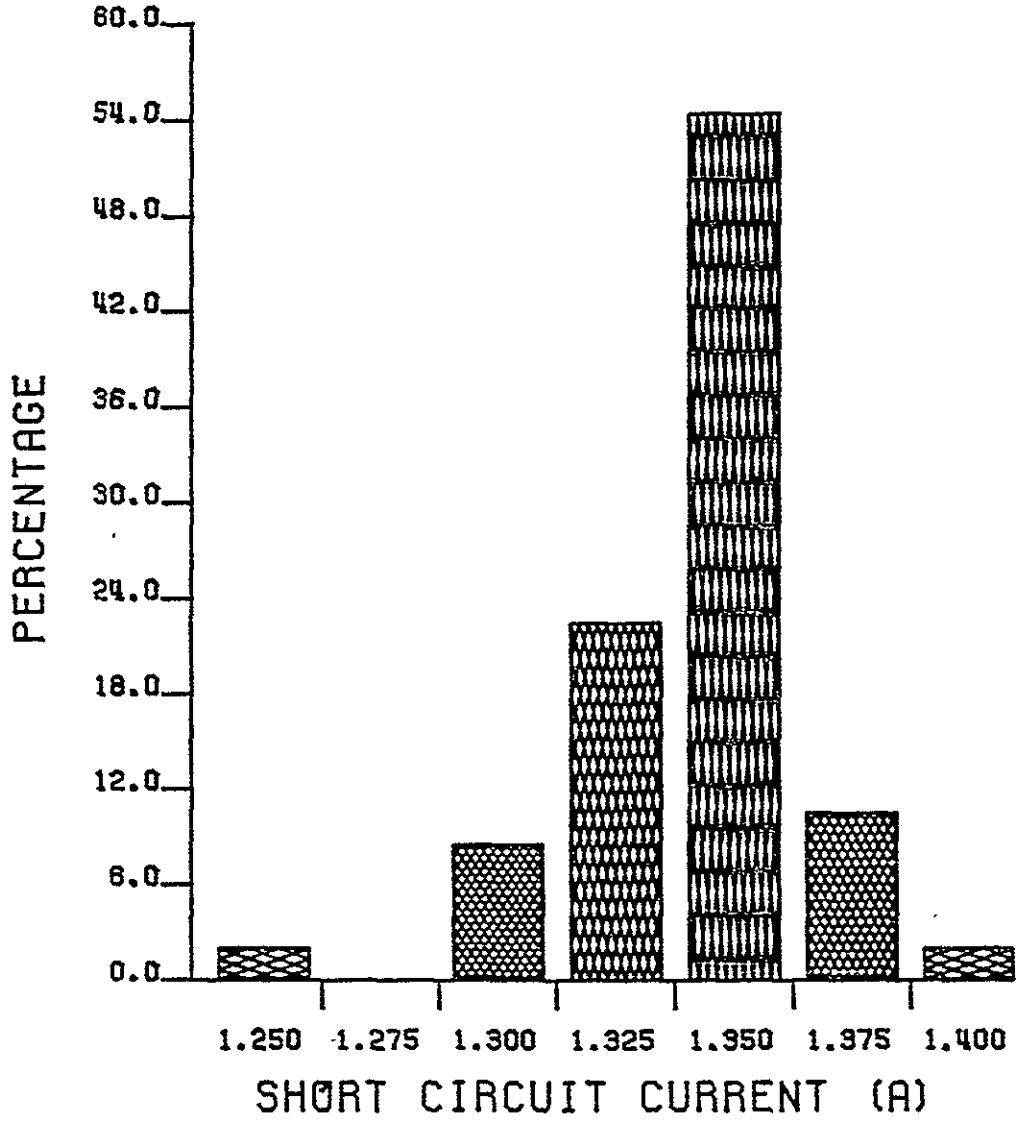

Figure A-7. Prestress Distribution of I_{sc}, Type G.

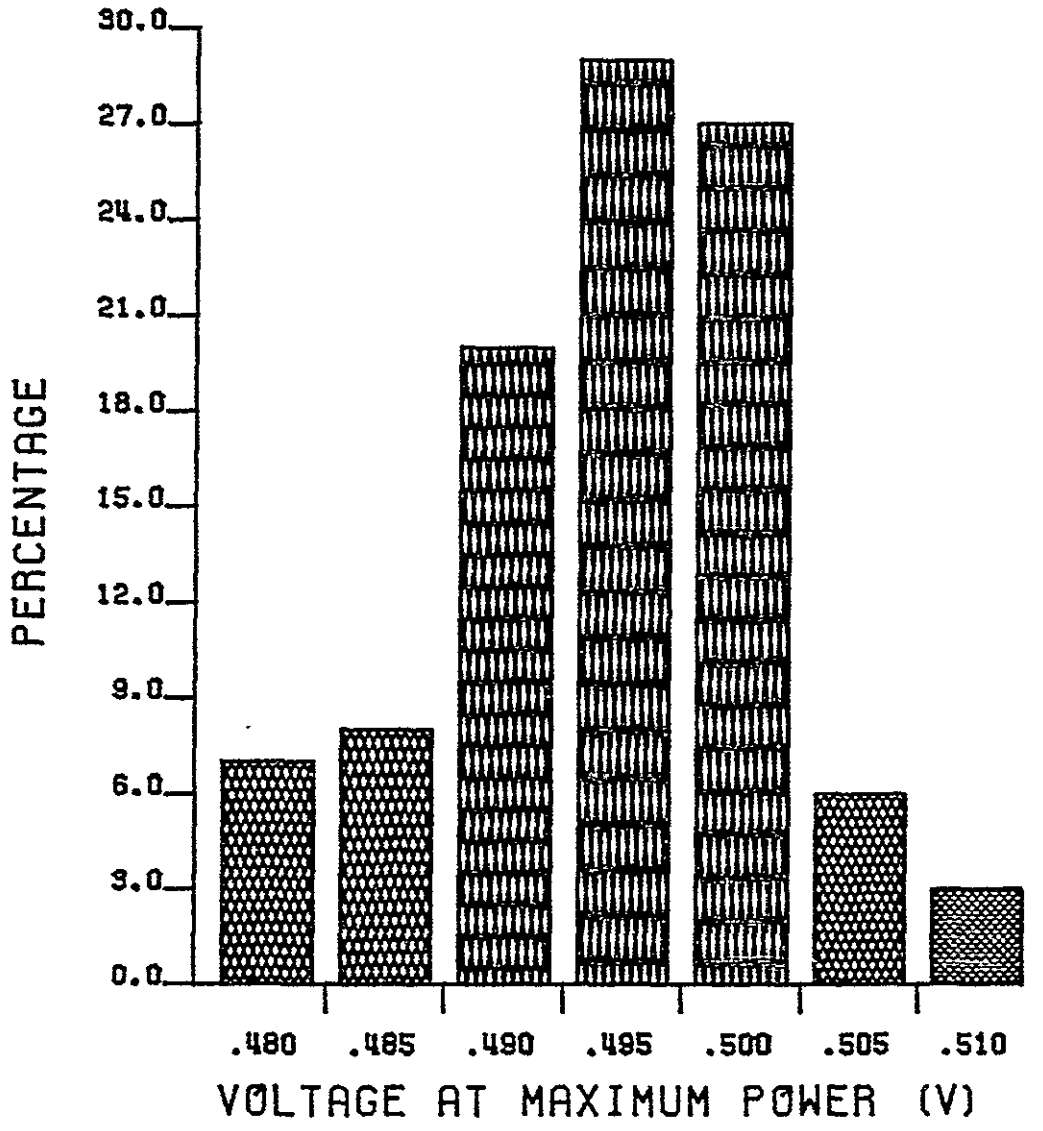

Figure A-8. Prestress Distribution of V_m, Type G.

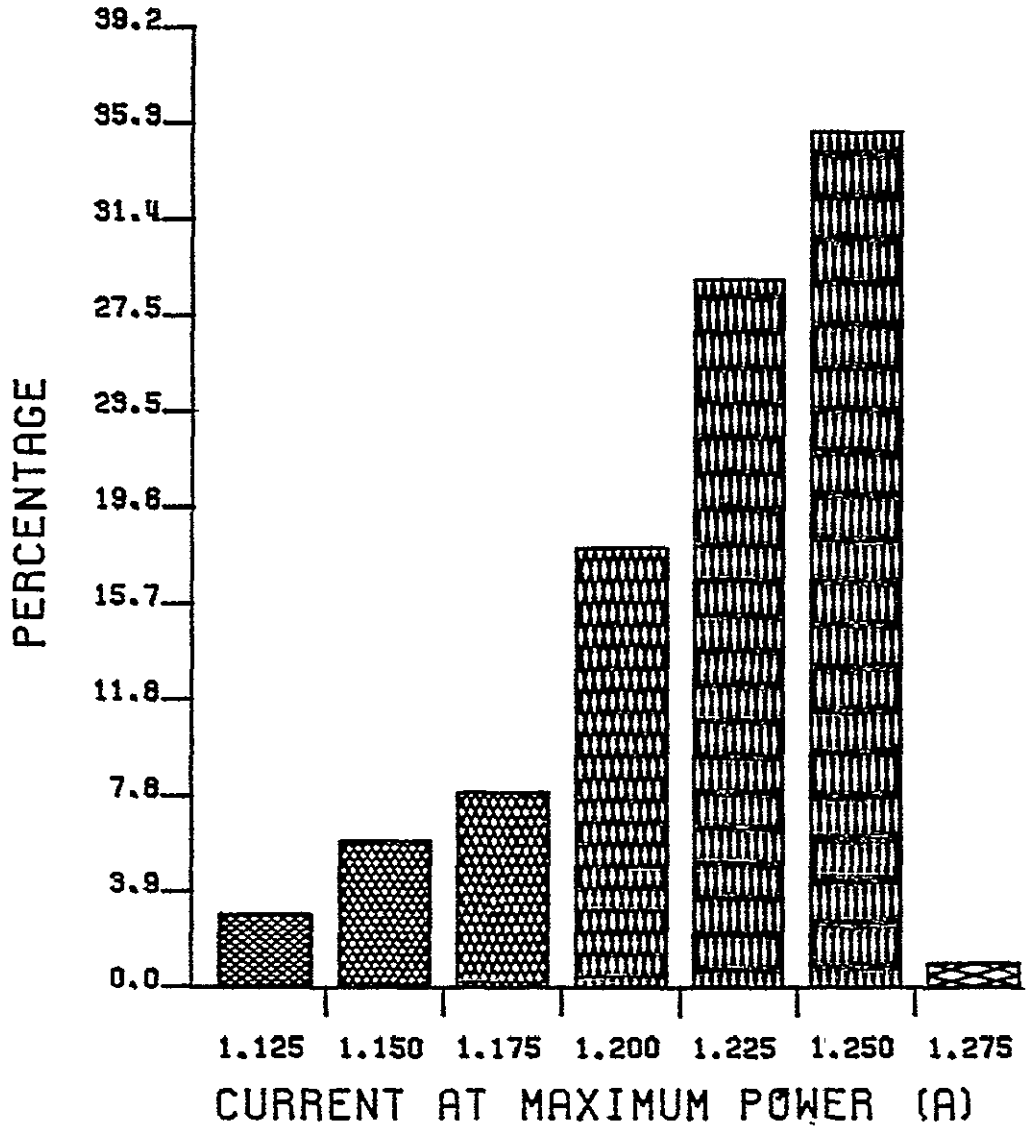

Figure A-9. Prestress Distribution of I_m, Type G.

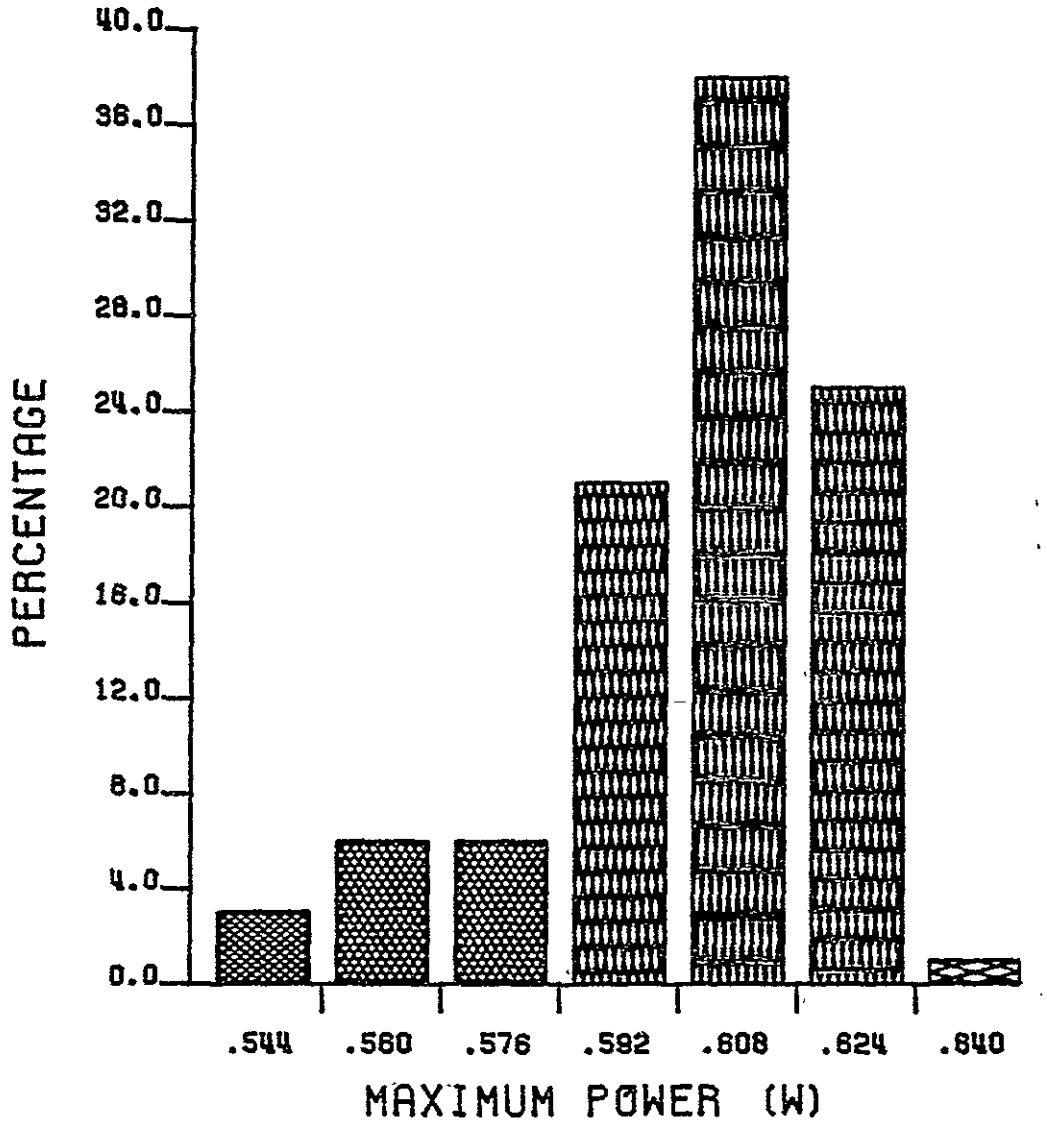

Figure A-10. Prestress Distribution of P_m, Type G.